

1  
2  
3  
4  
5  
6  
7  
8  
9  
10  
11  
12  
13  
14  
15  
16  
17  
18  
19  
20  
21  
22  
23  
24  
25

DR. RENE MANUEL VAN DER ZANDE (Orcid ID : 0000-0001-7321-0971)

DR. DOROTHEA BENDER-CHAMP (Orcid ID : 0000-0002-1279-7091)

Article type : Primary Research Articles

**Paradise lost: End-of-century warming and acidification under business-as-usual emissions have severe consequences for symbiotic corals**

Running Title: End-of-century coral reefs

Rene M van der Zande<sup>1,2</sup>, Michelle Achlatis<sup>1,2</sup>, Dorothea Bender-Champ<sup>1,2</sup>, Andreas Kubicek<sup>1,2</sup>, Sophie Dove<sup>1,2</sup>, Ove Hoegh-Guldberg<sup>1,2,3</sup>

<sup>1</sup>Coral Reef Ecosystems Lab, School of Biological Sciences, The University of Queensland, St. Lucia, QLD 4072, Australia, <sup>2</sup>Australian Research Council Centre of Excellence for Coral Reef Studies, The University of Queensland, St. Lucia, QLD 4072, Australia, <sup>3</sup>Global Change Institute, The University of Queensland, St. Lucia, QLD 4072, Australia

Corresponding author: Rene M van der Zande, Coral Reef Ecosystems Lab, School of Biological Sciences, The University of Queensland, St. Lucia, QLD 4072, Australia. Email: [rene.vanderzande@uq.net.au](mailto:rene.vanderzande@uq.net.au). ORCID iD: 0000-0001-7321-0971

This is the author manuscript accepted for publication and has undergone full peer review but has not been through the copyediting, typesetting, pagination and proofreading process, which may lead to differences between this version and the [Version of Record](#). Please cite this article as [doi: 10.1111/GCB.14998](https://doi.org/10.1111/GCB.14998)

This article is protected by copyright. All rights reserved

26 **Keywords:** climate change, coral bleaching, warming, acidification, RCP8.5, calcification,  
27 photosynthesis, *Symbiodinium*

28

## 29 **Abstract**

30 Despite recent efforts to curtail greenhouse gas emissions, current global emission trajectories  
31 are still following the business-as-usual RCP8.5 emission pathway. The resulting ocean warming  
32 and acidification have transformative impacts on coral reef ecosystems, detrimentally affecting  
33 coral physiology and health, and these impacts are predicted to worsen in the near future. In this  
34 study, we kept fragments of the symbiotic corals *Acropora intermedia* (thermally sensitive) and  
35 *Porites lobata* (thermally tolerant) for 7 weeks under an orthogonal design of predicted end-of-  
36 century RCP8.5 conditions for temperature and  $p\text{CO}_2$  (3.5 °C and 570 ppm above present-day  
37 respectively) to unravel how temperature and acidification, individually or interactively,  
38 influence metabolic and physiological performance. Our results pinpoint thermal stress as the  
39 dominant driver of deteriorating health in both species because of its propensity to destabilize  
40 coral-dinoflagellate symbiosis (bleaching). Acidification had no influence on metabolism but had  
41 a significant negative effect on skeleton growth, particularly when photosynthesis was absent  
42 such as in bleached corals or under dark conditions. Total loss of photosynthesis after bleaching  
43 caused an exhaustion of protein and lipid stores and collapse of calcification that ultimately led  
44 to *A. intermedia* mortality. Despite complete loss of symbionts from its tissue, *P. lobata*  
45 maintained small amounts of photosynthesis and experienced a weaker decline in lipid and  
46 protein reserves that presumably contributed to higher survival of this species. Our results  
47 indicate that ocean warming and acidification under business-as-usual  $\text{CO}_2$  emission scenarios  
48 will likely extirpate thermally-sensitive coral species before the end of the century, while  
49 slowing the recovery of more thermally-tolerant species from increasingly severe mass coral  
50 bleaching and mortality. This could ultimately lead to the gradual disappearance of tropical coral  
51 reefs globally, and a shift on surviving reefs to only the most resilient coral species.

52

## 53 **Introduction**

54 Oceans are warming and acidifying rapidly due to anthropogenic CO<sub>2</sub> and other greenhouse gas  
55 (GHG) emissions. As a result, marine ecosystems are changing (Hoegh-Guldberg et al., 2014),  
56 and coral reefs are among the ecosystems most urgently threatened (Hughes et al., 2017).  
57 Despite recent success in stabilizing the global increase in GHG emissions between 2014 and  
58 2016 (1.8% had dropped to 0.4% increase per year), GHG emission rates are currently back at  
59 2007-2013 levels (Jackson et al., 2017; Le Quéré et al., 2018; Peters et al., 2017) and tracking  
60 the high emission, ‘business-as-usual’ representative concentration pathway (RCP) 8.5 scenario.  
61 Irrespective of our efforts to curtail GHG emissions, the lagging persistence of CO<sub>2</sub> in the  
62 atmosphere will cause increased frequency and intensity of heat stress over the coming decades  
63 (Hoegh-Guldberg et al., 2014), and reefs worldwide will likely start experiencing annual  
64 bleaching outside of El Niño years (van Hooidonk et al., 2016).

65 Heat stress from warming oceans disrupts the symbiosis between the photosynthetic  
66 dinoflagellate endosymbionts (Symbiodiniaceae) and the coral host, resulting in expulsion of the  
67 endosymbiont from the coral tissue. The sensitivity of corals to heat stress depends on several  
68 abiotic factors such as the magnitude, rate of change, and duration of the thermal anomalies  
69 (Hughes et al., 2017), the thermal history (Grottoli et al., 2014), and potential interaction with  
70 other environmental factors (Courtney et al., 2017; Wolff, Mumby, Devlin, & Anthony, 2018).  
71 Additionally, biotic factors such as *Symbiodiniaceae* type(s) hosted (Berkelmans & van Oppen,  
72 2006; Fitt et al., 2009; Manzello et al., 2018), coral identity (Guest et al., 2016; Hoadley et al.,  
73 2019), coral microbiome composition (Ziegler et al., 2019; Ziegler, Seneca, Yum, Palumbi, &  
74 Voolstra, 2017), heterotrophic capacity (Ferrier-Pagès, Sauzéat, & Balter, 2018; Grottoli,  
75 Rodrigues, & Palardy, 2006) and skeleton morphology (Loya et al., 2001) lead to differences in  
76 thermal tolerance between coral species.

77 Healthy corals rely heavily on autotrophic carbon from their dinoflagellate symbionts for their  
78 daily metabolic needs (Grottoli et al., 2006; Muscatine, McCloskey, & Marian, 1981). Bleaching  
79 greatly reduces photosynthetic rates and hence the amount of photosynthetic carbon translocated  
80 to the coral host (Grottoli et al., 2006). The decline in autotrophy can be partly compensated by  
81 heterotrophy (Grottoli et al., 2006; Hughes, Grottoli, Pease, & Matsui, 2010; Levas et al., 2016;  
82 Palardy, Rodrigues, & Grottoli, 2008) and the catabolism of lipid or protein stores (Anthony,  
83 Hoogenboom, Maynard, Grottoli, & Middlebrook, 2009; Grottoli, Rodrigues, & Juarez, 2004;

84 Schoepf et al., 2015). However, prolonged bleaching may deplete stored energy reserves, leading  
85 to reduced metabolic activity and growth, and ultimately increased mortality (Anthony et al.,  
86 2009; Grottoli et al., 2014; Rodrigues & Grottoli, 2007).

87 At the same time, the dissolution of atmospheric CO<sub>2</sub> in the ocean changes the carbonate  
88 chemistry and decreases the seawater pH and aragonite saturation state ( $\Omega_{\text{ARAG}}$ ). Ocean  
89 acidification (OA) and declining  $\Omega_{\text{ARAG}}$  may affect corals by increasing bleaching susceptibility  
90 and holobiont productivity (Anthony, Kline, Diaz-Pulido, Dove, & Hoegh-Guldberg, 2008; but  
91 see Hoadley et al., 2016; Schoepf et al., 2013) and reducing nutrient uptake efficiency (Godinot,  
92 Houlbrèque, Grover, Ferrier-Pagès, & Larsen, 2011). More importantly, and although in some  
93 cases effects are minimal (e.g. Schoepf et al., 2013), a large body of literature has demonstrated  
94 that acidification reduces several key metrics of coral calcification such as skeleton  
95 microstructure (Cohen, McCorkle, de Putron, Gaetani, & Rose, 2009; Drenkard et al., 2013;  
96 Tambutté et al., 2015), linear extension rates (Crook, Cohen, Rebolledo-Vieyra, Hernandez, &  
97 Paytan, 2013) and overall CaCO<sub>3</sub> deposition (Edmunds, Brown, & Moriarty, 2012; Marubini,  
98 Ferrier-Pagès, Furla, & Allemand, 2008), while increasing skeleton porosity (Fantazzini et al.,  
99 2015; Tambutté et al., 2015). Ecologically, poorly developed coral skeletons lead to higher reef  
100 erosion and storm susceptibility (Manzello et al., 2008; Marshall, 2000), reduced capacity to  
101 compete for growing space (Darling, Alvarez-Filip, Oliver, McClanahan, & Côté, 2012) and the  
102 inability to keep up with sea level rise (van Woerik, Golbuu, & Roff, 2015).

103 Although it is known that elevated temperature and OA together impact coral health, metabolism  
104 and skeleton formation, the underlying interactive mechanisms of these factors is crucial in the  
105 assessment of the impact and magnitude of future changes (Bay, Rose, Logan, & Palumbi, 2017;  
106 Dove et al., 2013; Schoepf et al., 2019). The number of studies investigating the individual and  
107 combined effects of temperature and  $p\text{CO}_2$  in an orthogonal design has steadily increased in  
108 recent years (Büscher, Form, & Riebesell, 2017; Edmunds et al., 2012; Reynaud et al., 2003;  
109 Schoepf et al., 2013). However, not many orthogonal studies address extreme warming and  
110 acidification conditions (Hoadley et al., 2016) such as under the RCP8.5 emission scenario,  
111 which predicts a rise of approximately +3.5 °C and +570  $\mu\text{atm}$  CO<sub>2</sub> for non-El Niño years by  
112 2100 compared to present-day levels (Meinshausen et al., 2011; van Vuuren et al., 2011).  
113 Importantly, most studies employed static elevations of temperature and CO<sub>2</sub>, thereby losing the

114 diel and seasonal environmental cycles and variability of a natural system. Natural fluctuations in  
115 temperature and CO<sub>2</sub> significantly alter coral responses, and are often found to increase  
116 resilience to thermal and acidification stress (Chan & Eggins, 2017; Comeau, Edmunds, Spindel,  
117 & Carpenter, 2014; Jiang et al., 2019; Safaie et al., 2018). Using a novel system to manipulate  
118 warming and acidification, modelled on high-resolution present-day baselines, our study  
119 maintained this variability which is imperative to investigating organismal response to  
120 environmental changes (Rivest, Comeau, & Cornwall, 2017).

121 The present study therefore examines how warming and acidification under RCP8.5 may affect  
122 physiological parameters indicative of long and short-term coral health in two common reef-  
123 building coral species. *Acropora intermedia* and *Porites lobata* were selected as model species  
124 because of their contrasting life-history strategies and tolerance to environmental stress (Darling,  
125 McClanahan, & Côté, 2013; Levas, Grottoli, Hughes, Osburn, & Matsui, 2013). In an orthogonal  
126 design that respects diel and seasonal variability, present-day and end-of-century summer levels  
127 of temperature and pCO<sub>2</sub> were simulated over seven weeks. The chosen physiological parameters  
128 (long-term CaCO<sub>3</sub> deposition and skeleton extension, day and night calcification, photosynthetic  
129 and respiration rates, tissue lipid and protein reserves, bleaching and mortality) each give  
130 specific insights into organismal functioning, and collectively provide an ecophysiological  
131 framework for explaining future coral reef trajectories under climatic changes.

132

## 133 **Materials and methods**

### 134 *Experimental design*

135 Fragments of *Acropora intermedia* (Brook, 1891) and *Porites lobata* (Dana, 1846) were  
136 collected in November 2014 from Harry's Bommie on the leeward reef slope of Heron Island  
137 Reef (23°27'34" S 151°55'45" E) on the Southern Great Barrier Reef at 5 m water depth (Fig.  
138 1a). Samples were transported back to the Heron Island Research Station, where *A. intermedia*  
139 branch tips were trimmed to 5 cm length and suspended upright in 35 L outdoor glass aquaria  
140 using fishing line. Cores (30 mm diameter) were drilled from *P. lobata* colonies using a  
141 pneumatic underwater drill and cut to 2 cm height. In this way, a total of 96 fragments per  
142 species were collected from 8 adult colonies at least 10 m apart, with 10-14 fragments collected

143 per colony. Aquaria were covered with blue filters (Lee Filter #131 Marine Blue Filter,  
144 Hampshire, England) to replicate light conditions on the reef slope at 5 m water depth (Dove et  
145 al., 2013), and were equipped with a small powerhead (Hydor Koralia nano 900, HYDOR srl,  
146 Bassano del Grappa, Italy) for gentle water circulation (900 L h<sup>-1</sup>). Coral fragments fully  
147 recovered from sampling damage under untreated flow-through seawater for two weeks.  
148 Thereafter, treatment water from the sumps was gradually introduced and mixed with untreated  
149 seawater in 25% increments per week (to obtain 25, 50, 75 and 100% treatment water) until full  
150 treatment conditions were reached (December 3-27, 2014). Corals were then kept under 100%  
151 treatment conditions for 7 weeks over Austral summer, after which physiological measurements  
152 took place.

153 Temperature and  $p\text{CO}_2$  treatments were established using a computer-controlled simulation  
154 system in which different levels of warming and acidification can be achieved (for a detailed  
155 description of the system see Dove et al., (2013) as well as Achlatis et al. (2017) Supplementary  
156 Material). Treatment conditions were created as offsets to a variable temperature and  $p\text{CO}_2$   
157 baseline, established by CSIRO and the NOAA Pacific Marine Environment Laboratory Ocean  
158 Program using two- or three-hourly measurements over the previous summer at a reference  
159 location (Harry's Bommie) on Heron Island (Fig. S1, Fig. S2 in Supporting Information). This  
160 approach carefully preserved natural diel and seasonal fluctuations in temperature and  $p\text{CO}_2$ .  
161 Such variability is crucial because corals respond differently to static or variable environments  
162 (Rivest et al., 2017; Wahl, Saderne, & Sawall, 2016). Temperature and  $p\text{CO}_2$  were continuously  
163 maintained and monitored in individual 8000 L sumps (turnover rate 4-6 hours) using heater-  
164 chillers and gas injection (Achlatis et al., 2017; Dove et al., 2013). Four treatments were set up  
165 based on GHG emission trajectory RCP8.5 (IPCC 2013) for temperature and  $p\text{CO}_2$   
166 concentrations:

- 167 1. **Control.** Served as the baseline for all other modeled treatments; replicated present-day  
168 (PD) conditions for temperature and  $p\text{CO}_2$  at the reference site.
- 169 2. **Elevated  $p\text{CO}_2$ .** Increased only  $p\text{CO}_2$  concentrations while maintaining PD temperature  
170 levels. Conditions were increased to those typical of an average end-of-century non-El  
171 Niño year under RCP8.5 scenarios ( $570 \pm 11 \mu\text{atm}$  above PD levels).

172 3. **Elevated T.** Increased only temperature as specified by the above scenario (3.5 °C above  
173 PD levels) while maintaining PD  $p\text{CO}_2$  levels.

174 4. **Elevated T/ $p\text{CO}_2$ .** Increased both temperature and  $p\text{CO}_2$  concentration according to the  
175 same RCP8.5 scenario.

176 Treatment water was pumped from the sumps through the downstream aquaria ( $n = 2$  per  
177 treatment per species) containing the corals at  $0.8 \text{ L min}^{-1}$  (aquarium water turnover 30-40  
178 minutes). Light intensity inside the downstream aquaria was monitored using submersible light  
179 loggers (Odyssey Dataflow Systems). Seawater pH was measured continuously (InPro4501 VP  
180 X, Mettler Toledo, Victoria, Australia) in the downstream aquaria (Fig. S3), and temperature  
181 (Table 1, Fig. S1) was logged every 10 minutes (HOBO Pendant temperature loggers, Onset,  
182 Bourne, USA). Average PD and RCP8.5 temperatures were  $27.5 \text{ °C}$  and  $30.5 \text{ °C}$  respectively  
183 (Table 1). The maximum monthly mean (MMM) temperature for Heron Island is  $27.3 \text{ °C}$   
184 (Berkelmans, 2002), and degree heating weeks (DHW) started accumulating at  $\text{MMM} + 1 \text{ °C}$   
185 ( $28.3 \text{ °C}$ ). In the RCP8.5 and PD temperature treatments, this point was reached after December  
186 25<sup>th</sup> 2014 and January 27<sup>th</sup> 2015 respectively. Water samples for total alkalinity (TA) were  
187 collected weekly at midday and midnight in the downstream aquaria. TA was determined by  
188 Gran titration after Dickson et al. (2003) (Mettler-Toledo T50 titrator, Mettler-Toledo,  
189 Greifensee, Switzerland). TA values from these measurements were used to calculate  $p\text{CO}_2$  and  
190 aragonite saturation ( $\Omega_{\text{ARAG}}$ ) values in the downstream aquaria (Table 1).

191  
192 Table 1. Treatment design and reference experimental conditions (mean  $\pm$  sd) in the downstream  
193 aquaria during the 7-week experimental period. Seawater conditions were created in upstream  
194 sumps before being pumped through downstream aquaria containing the corals. Weekly  
195 aquarium temperature averages and measured TA and pH values were used to calculate  
196 downstream  $\Omega_{\text{ARAG}}$  and  $p\text{CO}_2$  using the program CO2SYS (version 2.1).

Experimental design		Downstream aquarium conditions					
Treatment	Temperature level	$p\text{CO}_2$ level	T (°C)	$p\text{CO}_2$ ( $\mu\text{atm}$ )	Total alkalinity ( $\mu\text{mol kg}^{-1}$ )	pH <sub>NBS</sub>	$\Omega_{\text{ARAG}}$
Control (PD)	PD	PD	$27.5 \pm 1.6$	$490 \pm 99$	$2210 \pm 32$	$8.10 \pm 0.07$	$3.24 \pm 0.13$

Elevated $p\text{CO}_2$	PD	RCP8.5	$27.4 \pm 1.9$	$925 \pm 204$	$2218 \pm 39$	$7.87 \pm 0.08$	$2.18 \pm 0.10$
Elevated T	RCP8.5	PD	$30.4 \pm 1.8$	$524 \pm 162$	$2258 \pm 10$	$8.09 \pm 0.08$	$3.39 \pm 0.38$
Elevated T/ $p\text{CO}_2$	RCP8.5	RCP8.5	$30.8 \pm 2.0$	$890 \pm 47$	$2261 \pm 10$	$7.89 \pm 0.02$	$2.32 \pm 0.07$

197

198 As the possibility of coral mortality was anticipated during the experimental period, each  
 199 treatment was started with  $n = 24$  corals to maximize the number of potentially surviving corals  
 200 at the point of the physiological measurements. Twelve randomly selected fragments of either *A.*  
 201 *intermedia* or *P. lobata* were kept in each aquarium, with two aquaria per species for each  
 202 treatment. Coral fragments were randomly assigned to aquaria, and placement of the aquaria was  
 203 randomized such as to receive one of four treatment conditions. Corals were rotated between  
 204 aquaria of the same treatment every fourth day in order to eliminate potential tank or positional  
 205 effects (e.g. light variations) (Hughes et al., 2010; Levas et al., 2013; Schoepf et al., 2014).  
 206 Corals were always rotated in the same cohort to enable cohort effects to be calculated and  
 207 compared. Aquaria were emptied and cleaned before rotation to prevent any carry-over effects  
 208 (e.g. pathogens) between cohorts. All corals were supplementary fed thawed *Artemia* (~250 mg  
 209 per aquarium) daily after sunset. Water flow was interrupted for one hour during the feeding,  
 210 while powerheads were kept on to maintain a gentle mixing. Bleaching and mortality were  
 211 recorded every second day starting at the initiation of the treatment increments. Onset of  
 212 bleaching was determined when fragments dropped two colour codes on the Coral Watch coral  
 213 health chart compared to their initial colour code (Siebeck, Marshall, Klüter, & Hoegh-Guldberg,  
 214 2006). Fragments were kept in the treatments as long as alive even when fully bleached.  
 215 Mortality was determined as visual loss of all tissue, absence of tentacle extension at night and  
 216 subsequent algae overgrowth. Dead corals were removed from the aquaria and not included in  
 217 subsequent measurements.

218

### 219 *Metabolic measurements*

220 Metabolic oxygen flux was measured over light-dark cycle incubations to calculate  
 221 photosynthetic and respiratory rates. Corals ( $n = 8$  per treatment) were placed in 250 ml acrylic  
 222 chambers containing  $0.45 \mu\text{m}$  filtered seawater (FSW) from the respective treatments and  
 223 equipped with magnetic stirrers for water circulation. Oxygen content of the FSW was reduced



224 to approximately 60% air saturation by nitrogen gas bubbling, which may have slightly affected  
225 the seawater carbonate chemistry. Chambers were sealed with acrylic lids equipped with oxygen  
226 sensors, and a water bath mimicked the temperature of the respective treatments (Julabo F33ME  
227 refrigerated/heating circulator, Seelbach, Germany). Seawater oxygen content was logged at 15  
228 second intervals during 30/30-minute light/dark cycles (PreSens OXY-10 mini oxygen meter,  
229 PreSens, Regensburg, Germany). Net photosynthesis ( $P_{NET}$ ) and dark respiration ( $R_{DARK}$ ) rates  
230 were calculated from the oxygen measurements during the light period and after 20 minutes of  
231 dark acclimation respectively.  $P_{NET}:R_{DARK}$  ratios were calculated to gauge holobiont potential for  
232 remaining net photosynthetic over a 24-hour period, based on a 12.5/11.5-hour light/dark period.  
233 Incubations were done under  $320 \mu\text{mol quanta m}^{-2} \text{ s}^{-1}$  (mean summer maximum daily reef slope  
234 light intensity) using Aqua Medic Ocean Lights, Bissendorf, Germany; 1 x 250 W metal halide  
235 lamp and 2 x 24 W aqualine T5 fluorescent bulbs.

236

### 237 *Measurements of skeletogenesis*

238 Three separate measurements of skeletogenesis were performed. Two measurements integrated  
239 skeleton growth over the experimental period: long-term average  $\text{CaCO}_3$  deposition ( $G_{DW}$ ) and  
240 skeleton volume change ( $\Delta\text{Volume}$ ). One measurement recorded instantaneous, end-of-treatment  
241 day and night  $\text{CaCO}_3$  accretion ( $G_{TA}$ ) under the conditions of summer thermal maximum.  $G_{DW}$   
242 was defined as the rate of  $\text{CaCO}_3$  accretion calculated from the initial and endpoint dry weights  
243 of the treatment fragments averaged over the experimental period (Eq. 1).

$$244 \quad G_{DW} (\text{mg CaCO}_3 \text{ cm}^{-2} \text{ d}^{-1}) = \frac{(DW_{end} - DW_{initial})}{(\text{mean SA}_{initial} \cdot \text{days})} \quad \text{Eq. 1}$$

245 In order not to sacrifice the treatment corals, their initial dry weights ( $DW_{initial}$ ) were inferred  
246 from their initial buoyant weights ( $BW_{initial}$ ). For this, a separate subset of coral fragments ( $n = 8$   
247 and  $n = 20$  for *A. intermedia* and *P. lobata* respectively) were collected at the start of the  
248 experiment. Fragments in this subset were buoyant weighed, coral tissue was removed and  
249 skeletons were treated with 10% hypochlorite solution for 24 hours to remove remaining organic  
250 material (Gaffey & Bronnimann, 1993), and dried and reweighed for skeleton  $DW_{initial}$ . The  
251 relationship between skeleton buoyant and dry weights is determined the skeleton and seawater  
252 density (Spencer Davies, 1989). Skeletal density was assumed not to vary significantly within a

253 species, justified by the selection of nubbins of similar orientation and position within colonies  
 254 exposed to similar light conditions. This rendered a linear relationship between the  $BW_{initial}$  and  
 255  $DW_{initial}$  of the subset fragments (Eq. 2,  $r^2 = 0.9952$  and Eq. 3,  $r^2 = 0.9941$  for *A. intermedia* and  
 256 *P. lobata* respectively), which was used to infer  $DW_{initial}$  of the treatment corals (Spencer Davies,  
 257 1989).

$$258 \quad DW_{initial}(A. intermedia) = (1.5296 \cdot BW_{initial}) \quad \text{Eq. 2}$$

$$259 \quad DW_{initial}(P. lobata) = (1.5779 \cdot BW_{initial}) \quad \text{Eq. 3}$$

261 Initial mean skeletal densities and volumes of the treatment fragments were  $3.01 \text{ g cm}^{-3}$  and  $0.66$   
 262  $\text{cm}^3$  for *A. intermedia* and  $2.83 \text{ g cm}^{-3}$  and  $7.30 \text{ cm}^3$  for *P. lobata*.  $G_{DW}$  of the treatment  
 263 fragments was calculated from their inferred initial ( $DW_{initial}$ ) and measured end-point ( $DW_{end}$ )  
 264 dry weights (Eq. 3). Initial and end-point skeleton volumes were calculated from skeleton  
 265 buoyant and dry weights, and average daily rates of volume change between the start and end of  
 266 the experiment were calculated according to Eq. 4 (adapted from Spencer Davies, (1989)).

$$267 \quad \Delta Volume \text{ (mm}^3 \text{ cm}^{-2} \text{ d}^{-1}) = \frac{((DW_{end} - BW_{end}) - (DW_{initial} - BW_{initial}))}{(\Delta \text{ days} \cdot \delta_{SW} \cdot \text{mean } SA_{initial})} \cdot 1000 \quad \text{Eq. 4}$$

269 End-of-treatment instantaneous calcification rates ( $G_{TA}$ ,  $n = 8$  per treatment) were determined  
 270 under day and night conditions using the TA anomaly method (Chisholm & Gattuso, 1991). TA  
 271 change was measured over separate 1-hour light and dark incubations at physiological day  
 272 (11:00 - 12:00) and night (21:30 - 22:30) time to ensure natural light and dark rhythms.  
 273 Incubations were done under the same settings as the metabolic oxygen flux measurements.  
 274 Water samples for TA determination were collected before (triplicate sample from the filtered  
 275 batch treatment water) and after each incubation from the individual chamber. TA was  
 276 determined by Gran titration as above, and used to calculate day and night  $G_{TA}$  rates (Eq. 5).

$$277 \quad G_{TA} \text{ (}\mu\text{mol CaCO}_3 \text{ cm}^{-2} \text{ h}^{-1}) = \left( \frac{\Delta TA \text{ (}\mu\text{mol)}}{2 \cdot SA_{end} \text{ (cm}^2) \cdot \text{time (h)}} \right) \cdot Vol \text{ (L)} \quad \text{Eq. 5}$$

279

280 *Tissue parameters*

281 Tissue protein and lipid content (n = 8 per treatment) was measured at the end of the treatment  
282 period. Tissue was collected from the skeletons using a simple airbrush and 30 ml FSW. Half of  
283 the obtained mixture was stored at -20 °C for lipid analysis. The other half was centrifuged for  
284 mass separation at 4500 RPM for 5 minutes, and a 2 ml sample of the supernatant was kept for  
285 water-soluble host protein determination. The remaining pellet was washed with 5 ml FSW,  
286 centrifuged at 4500 RPM for 5 minutes for a total of three washes to clean the pellet from coral  
287 mucus, and then resuspended in 5 ml FSW for symbiont density determination by microscope  
288 hemocytometer counts.

289 Water-soluble host protein content was determined by differential absorbance at 235 and 280 nm  
290 using spectrometry (Spectra Max 2, Molecular Devices, Sunnyvale, California) (Whitaker &  
291 Granum, 1980). Lipids were measured using a modified protocol of Dunn et al. (2012). The  
292 frozen lipid sample was freeze-dried (ScanVac CoolSafe, LaboGene, Lillerød, Denmark), and  
293 dry material was dissolved in 5 ml 2:1 chloroform/methanol solution, vortexed and left overnight  
294 at 4°C to allow full lipid extraction. Next, the samples were centrifuged at 4000 RPM for 4  
295 minutes and the organic solvent was transferred into a clean tube. The remaining pellet was  
296 rinsed with 2 ml chloroform/methanol solution, and this solution was added to the original 5 ml  
297 after one hour at 4 °C. Next, 1 ml of 0.1 mol l<sup>-1</sup> KCl solution was added to the organic solvent,  
298 and left overnight at 4°C to allow separation of organic and aqueous phases. After careful  
299 removal of the aqueous phase, the remaining organic phase was washed with 5 ml 1:1  
300 methanol/MQ solution three times. Each wash was left overnight at 4°C for phase separation and  
301 subsequent removal of the aqueous phase. After the third wash the remaining organic solution  
302 was poured into a pre-weighed aluminum tray, left to evaporate, and reweighed for lipid  
303 quantification. The surface area covered by live coral tissue was calculated using the double  
304 waxing method (Veal, Carmi, Fine, & Hoegh-Guldberg, 2010) applied to bleached and dried  
305 skeletons.

306

307 *Statistical analyses*

308 The overall holobiont response for each species to the temperature and  $p\text{CO}_2$  treatments was  
309 analyzed using multivariate two-way analysis of similarities (ANOSIM) with 9999 permutations.  
310 All data was square root transformed and ranked similarities were calculated using Bray-Curtis  
311 similarities. Treatment responses were graphically represented using non-metric  
312 multidimensional scaling (nMDS). Multivariate analyses were done in PRIMER V6 (PRIMER-e,  
313 Auckland, New Zealand), and included all measured physiological variables: symbiont density,  
314  $P_{\text{NET}}$ ,  $R_{\text{DARK}}$ ,  $P_{\text{NET}}:R_{\text{DARK}}$ , averaged long-term  $\text{CaCO}_3$  accretion rates ( $G_{\text{DW}}$ ), skeleton volume  
315 increase, tissue lipid and protein content, and end-of-experiment light and dark calcification rates  
316 ( $G_{\text{TA}}$ ).

317 Further analysis of each individual physiological variable except the  $G_{\text{TA}}$  measurements was  
318 done using a nested two-factorial ANOVA design. The categorical factors temperature and  $p\text{CO}_2$   
319 had two levels each, PD and RCP8.5. Cohort was nested in the interaction of the factors to test  
320 for cohort-specific effects (Tolosa, Treignier, Grover, & Ferrier-Pagès, 2011), which were absent  
321 for all parameters tested. Measurements of  $G_{\text{TA}}$  were analyzed in a mixed three-factorial  
322 ANOVA, with temperature and  $p\text{CO}_2$  as between subjects factors, and Time (Day/Night) as the  
323 within subjects factor. Cohort effect in light and dark  $G_{\text{TA}}$  rates was analyzed separately in a  
324 preliminary analysis, whereby cohort response was nested in the interaction of the factors (Table  
325 S1). No between-cohort effects were found and samples from the duplicate cohorts per treatment  
326 were therefore pooled (Tremblay et al., 2012; Tremblay, Gori, Maguer, Hoogenboom, & Ferrier-  
327 Pagès, 2016; Underwood, 1997) for the  $G_{\text{TA}}$  analysis. Coral bleaching and survival curves were  
328 analyzed using a two-proportion z-test. All analyses were tested for violations of normality  
329 (Shapiro-Wilk test) and homogeneity of variances (Levene's test), and transformed where  
330 necessary using square-root or log transformation. Results were tested against the  $\alpha = 0.01$  level  
331 to reduce chances of a type-I error when assumptions were still violated after transformation  
332 (Underwood, 1997). In all other cases significance was tested against the  $\alpha = 0.05$  level. All  
333 factorial analyses were done with Statistica 13.2 (Statsoft, Tulsa, OK, USA).

334

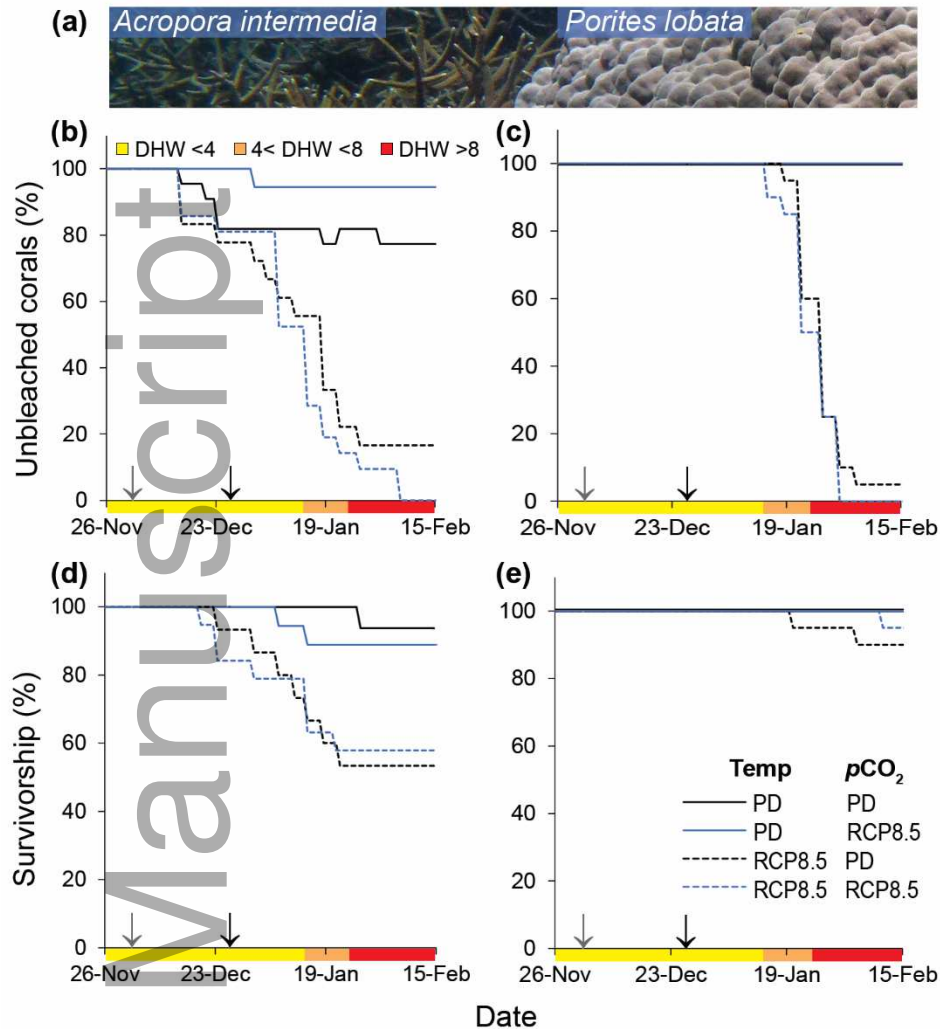
## 335 **Results**

### 336 *Bleaching and mortality*

337 Thermal stress regimes for the RCP8.5 temperature treatments were as follows: DHW < 4  
338 between December 25<sup>th</sup> and January 13<sup>th</sup>; 4 < DHW < 8 between January 14<sup>th</sup> and 24<sup>th</sup>; DHW > 8  
339 after January 24<sup>th</sup>, until a maximum of 15.6 °C weeks had been reached at the end of the  
340 experimental period on February 15<sup>th</sup> (Fig. 1). In the PD temperature treatments, thermal stress  
341 reached 0.5 °C weeks by the end of the experimental periods.

342 Bleaching of *A. intermedia* in the elevated temperature treatments started halfway through the  
343 treatment increment period. By the time full treatment was reached, 20% of specimens under  
344 elevated temperatures were visibly bleached, and the number of bleached corals continued to  
345 increase steadily (Fig. 1b). After seven weeks in the elevated T and elevated T/pCO<sub>2</sub> treatments,  
346 respectively 83% (z = 3.43, p < 0.001) and 100% (z = 4.42, p < 0.001) of *A. intermedia* had  
347 bleached. There was a low occurrence of *A. intermedia* bleaching in both PD temperature  
348 treatments irrespective of the pCO<sub>2</sub> concentration because of high baseline summer temperatures.  
349 Bleaching of *P. lobata* under both elevated temperature treatments started at approximately three  
350 weeks into full treatment (Fig. 1c). Respectively 95% (z = 5.79, p < 0.001) and 100% (z = 6.04,  
351 p < 0.001) of *P. lobata* specimens in the elevated T and T/pCO<sub>2</sub> bleached, while no significant *P.*  
352 *lobata* bleaching occurred under PD temperatures. Mortality in *A. intermedia* under elevated  
353 temperatures trailed the onset of bleaching by approximately 2 weeks (Fig. 1d). After seven  
354 weeks mortality reached 46.7% (z = 2.51, p = 0.012) and 42.1% (z = 2.29, p = 0.022) in the  
355 elevated T and T/pCO<sub>2</sub> treatments, respectively. No significant differences in *P. lobata* mortality  
356 were observed between treatments (Fig. 1e).

357



358

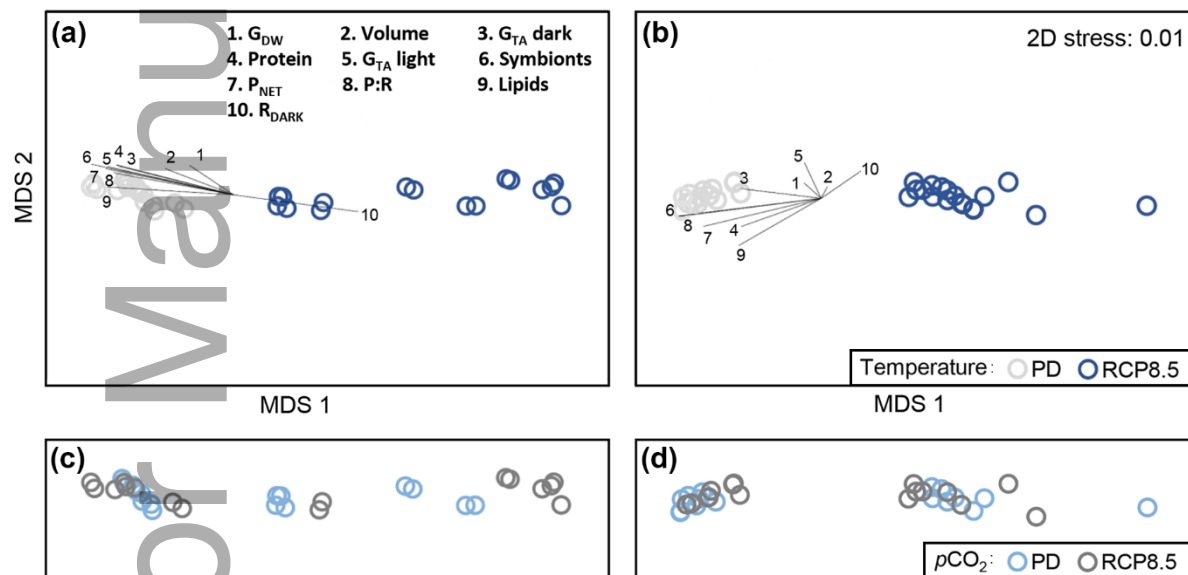
359 **Figure 1.** Bleaching and survival curves for *Acropora intermedia* (left panels) and *Porites lobata*  
 360 (right panels) during warming and acidification stress. Inset picture (a) shows co-occurring  
 361 colonies of the two species on Heron Island. Specimens were exposed to independent and  
 362 concurrent levels of temperature and  $pCO_2$  according to end-of-century RCP8.5 emission  
 363 scenarios over seven weeks. The percentage of unbleached (b,c) and dead (d,e) corals were  
 364 recorded every second day. The seven-week experimental period was preceded by four weeks of  
 365 step-wise treatment exposure (25% increments weekly). Grey (December 3, 2014) and black  
 366 (December 27, 2014) arrows depict the start of the step-wise introduction and full treatment  
 367 phases respectively. The colored horizontal bar represents the degree heating weeks (DHW; °C  
 368 weeks) reached in the elevated temperature treatments, throughout the experiment; yellow for

369 DHW < 4 (November 26<sup>th</sup> 2014 - January 13<sup>th</sup> 2015), orange for 4 < DHW < 8 (January 14<sup>th</sup> -  
370 24<sup>th</sup> 2015) and red for DHW > 8 (January 25<sup>th</sup> - February 15<sup>th</sup> 2015).

371

### 372 *Multivariate analyses*

373 Overall, the physiological response in *A. intermedia* (Fig. 2a) was strongly determined by the  
374 effect of elevated temperature (ANOSIM R = 0.878, p < 0.001), and less by elevated pCO<sub>2</sub>  
375 (ANOSIM R = 0.225, p = 0.011). The overall response of *P. lobata* was similar to *A. intermedia*,  
376 depending strongly on thermal stress (ANOSIM R = 1, p < 0.001) and less on acidification  
377 (ANOSIM R = 0.116, p = 0.043), consistent with the nMDS results (Fig. 2).



378

379 **Figure 2.** Non-metric multidimensional scaling (nMDS) plots showing similarities in overall  
380 holobiont response for *Acropora intermedia* (a) and *Porites lobata* (b) to differential temperature  
381 and pCO<sub>2</sub> treatments. Top panels show grouping based on response to warming, whereas bottom  
382 panels depict grouping based on acidification effects. Vector overlay depicts the proportional  
383 contribution of each biological variable (numbered) to the distribution.

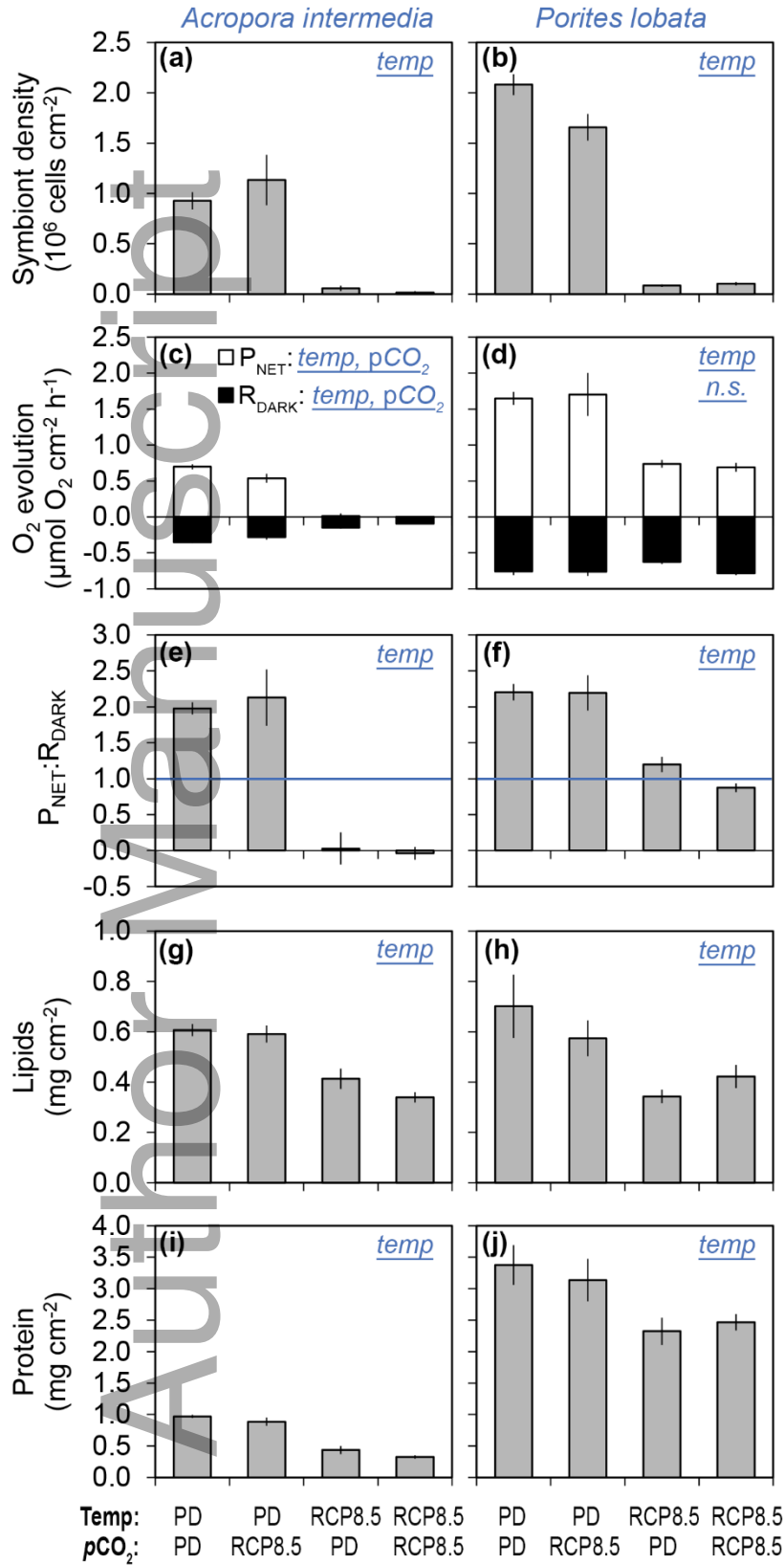
384

### 385 *Metabolic and tissue parameters*

386 Specimens of *A. intermedia* and *P. lobata* under heat stress contained significantly lower  
387 amounts of dinoflagellate symbionts in their tissue (Fig. 3). Irrespective of the level of  $p\text{CO}_2$ ,  
388 warming reduced symbiont concentrations by 28-fold in *A. intermedia* (main effect T;  $F_{1,24} =$   
389  $125.5$ ,  $p < 0.001$ ; Fig. 3a) and 20-fold in *P. lobata* (main effect T;  $F_{1,24} = 285.7$ ,  $p < 0.001$ ; Fig.  
390 3b). Rates of  $P_{\text{NET}}$  in *A. intermedia* (Fig. 3c) decreased when exposed to elevated temperature  
391 (main effect T;  $F_{1,24} = 262.0$ ,  $p < 0.001$ ) and  $p\text{CO}_2$  levels (main effect  $p\text{CO}_2$ ;  $F_{1,24} = 5.2$ ,  $p =$   
392  $0.032$ ), but not their interaction, with highest  $P_{\text{NET}}$  values being measured in the control  
393 treatment. Similarly,  $R_{\text{DARK}}$  rates in *A. intermedia* were governed by elevated temperature (main  
394 effect T;  $F_{1,24} = 106.5$ ,  $p < 0.001$ ) and elevated  $p\text{CO}_2$  levels individually (main effect  $p\text{CO}_2$ ;  $F_{1,24}$   
395  $= 12.0$ ,  $p = 0.002$ ). In *P. lobata*,  $P_{\text{NET}}$  (Fig. 3d) was affected by warming alone, dropping more  
396 than 50% in elevated temperature treatments (main effect T;  $F_{1,24} = 40.79$ ,  $p < 0.001$ ). No  
397 significant differences were found in  $R_{\text{DARK}}$  rates for *P. lobata*.  $P_{\text{NET}}:R_{\text{DARK}}$  ratios for *A.*  
398 *intermedia* (Fig. 3e) declined from  $1.98 \pm 0.08$  and  $1.84 \pm 0.14$  in the control and elevated  $p\text{CO}_2$   
399 treatments respectively, to approximately zero values at elevated temperatures, irrespective of  
400 the level of  $p\text{CO}_2$  (main effect T;  $F_{1,24} = 193.9$ ,  $p < 0.001$ ). Warming significantly reduced  
401  $P_{\text{NET}}:R_{\text{DARK}}$  ratios in *P. lobata* (Fig. 3f) irrespective of the level of  $p\text{CO}_2$ .  $P_{\text{NET}}:R_{\text{DARK}}$  ratios were  
402 above 2 in both PD temperature treatments, and dropped to  $1.20 \pm 0.11$  and  $0.87 \pm 0.06$  for  
403 elevated T and elevated T/ $p\text{CO}_2$  treatments respectively (main effect T;  $F_{1,24} = 64.93$ ,  $p < 0.001$ ).

404 Exposure to elevated temperatures decreased the tissue lipid concentration in both *A. intermedia*  
405 (main effect T;  $F_{1,24} = 48.02$ ,  $p < 0.001$ ) and *P. lobata* (main effect T;  $F_{1,24} = 10.50$ ,  $p = 0.003$ )  
406 while tissue lipid concentration was unaffected by acidification (Fig. 3g, h). Similarly, host  
407 protein concentrations in both coral species declined as a result of heat stress (main effect T;  $F_{1,24}$   
408  $= 111.7$ ,  $p < 0.001$  and main effect T;  $F_{1,24} = 9.410$ ,  $p = 0.005$  for *A. intermedia* and *P. lobata*  
409 respectively). Host protein concentrations in both species were unaffected by different levels of  
410  $p\text{CO}_2$  (Fig. 3i, j).



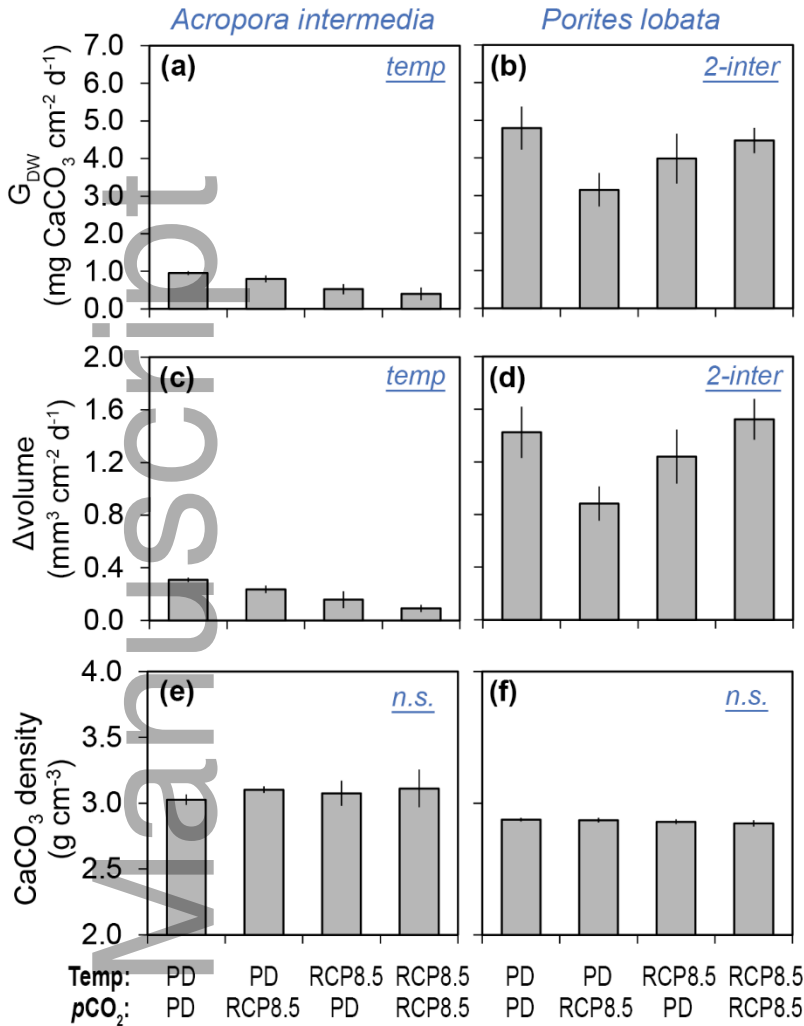


412 **Figure 3.** Parameters of photobiology and tissue composition (mean  $\pm$  SE) of *Acropora*  
413 *intermedia* (left panels) and *Porites lobata* (right panels) after exposure to different treatments of  
414 warming and acidification. Dinoflagellate symbiont density (a,b), photobiology (c-f) and tissue  
415 lipid (g,h) and protein content (i,j) were measured on corals (n = 8 per treatment) exposed for  
416 seven weeks to independent and concurrent levels of temperature and  $p\text{CO}_2$  according to end-of-  
417 century RCP8.5 projections. Horizontal blue lines in (e,f) at  $P_{\text{NET}}:R_{\text{DARK}} = 1$  depict the  
418 autotrophic break-even ratio. The blue text inside the panels indicates the absence (n.s. = no  
419 significance) or presence of significant main effects of warming (temp) and/or acidification  
420 ( $p\text{CO}_2$ ).

421

#### 422 *Skeletal accretion*

423 Long-term average rates of  $\text{CaCO}_3$  accretion ( $G_{\text{DW}}$ ) were differentially affected by warming and  
424 acidification in each species. In *A. intermedia*,  $G_{\text{DW}}$  declined after exposure to elevated compared  
425 to PD temperatures (main effect T;  $F_{1,24} = 14.30$ ,  $p = 0.001$ ), while it was unaffected by  
426 acidification (Fig. 4a). In *P. lobata*, exposure to elevated  $p\text{CO}_2$  reduced  $G_{\text{DW}}$  rates only under PD  
427 (Fig. 4b), and not under elevated temperatures (interactive effect  $T \times p\text{CO}_2$ ;  $F_{1,24} = 4.445$ ,  $p =$   
428  $0.046$ ). Skeleton volume of *A. intermedia* (Fig. 4c) increased less over time under warming,  
429 while it was unaffected by  $p\text{CO}_2$  levels (main effect T;  $F_{1,24} = 16.65$ ,  $p < 0.001$ ). In *P. lobata*,  
430 skeleton volume change was governed by an interactive effect of temperature and  $p\text{CO}_2$  (Fig.  
431 4d). Volume expansion was reduced by acidification under PD temperatures, but it was  
432 unaffected under elevated temperature levels (interactive effect  $T \times p\text{CO}_2$ ;  $F_{1,24} = 6.394$ ,  $p =$   
433  $0.018$ ). Despite the observed differences in volume change between warming and acidification  
434 scenarios in both species, skeleton density did not differ between the treatments (Fig. 4e, f).

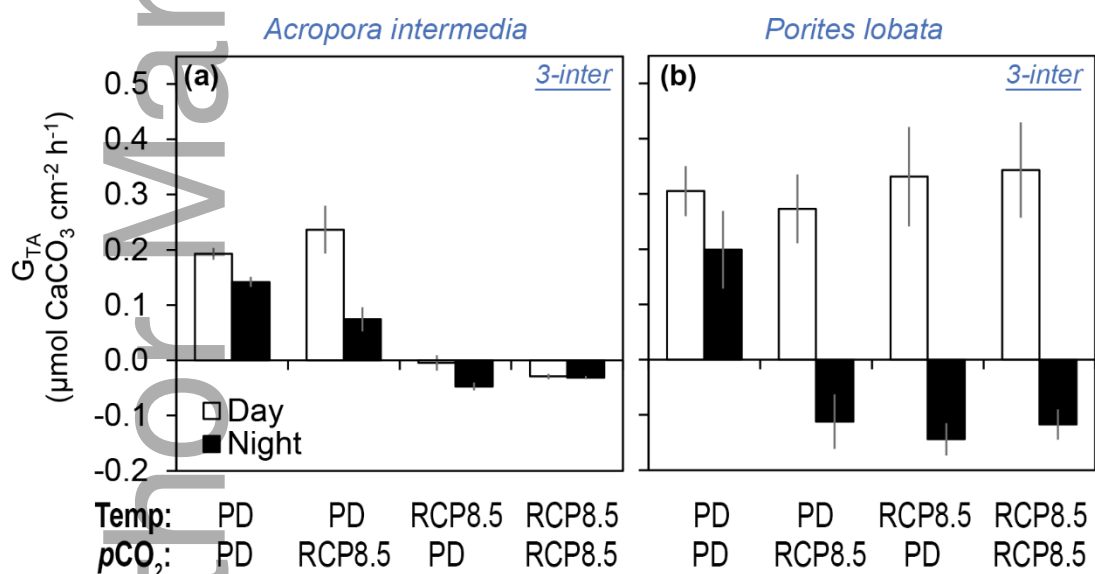


435

436 **Figure 4.** Parameters of long-term skeleton growth (mean ± SE) under different treatments of  
 437 warming and acidification for *Acropora intermedia* (left panels) and *Porites lobata* (right  
 438 panels). Seven-week averages of skeleton CaCO<sub>3</sub> accretion (G<sub>DW</sub>; a,b) and skeleton volume  
 439 expansion rates (c,d) were determined for corals exposed to independent and concurrent levels of  
 440 temperature and pCO<sub>2</sub> according to end-of-century RCP8.5 projections. Averages span the entire  
 441 period, including before the onset of bleaching. Skeleton density (e,f) was determined at the end  
 442 of the experimental period. The blue text inside the panels indicates the presence of significant  
 443 main effects of warming (temp) or 2-way interactive effects of warming and acidification (2-  
 444 inter).

445

446 End-of-treatment rates of calcification ( $G_{TA}$ ) in *A. intermedia* (Fig. 5a) were governed by a three-  
 447 way interaction between temperature,  $pCO_2$  and time of measurement (interactive effect Time  $\times$   
 448 T  $\times pCO_2$ ;  $F_{1,28} = 23.3$ ,  $p < 0.001$ ). When exposed to elevated  $pCO_2$ , daytime  $G_{TA}$  rates were  
 449 threefold higher than nighttime  $G_{TA}$  rates (Tukey HSD  $p < 0.001$ ). Warming decreased  $G_{TA}$  to  
 450 below zero levels irrespective of light or dark conditions (Tukey HSD  $p < 0.001$ ). When  
 451 measured under dark conditions, exposure to elevated temperature reduced  $G_{TA}$  rates more under  
 452 PD  $pCO_2$  compared to elevated  $pCO_2$  levels (Tukey HSD  $p < 0.001$ ). Likewise,  $G_{TA}$  rates in *P.*  
 453 *lobata* (Fig. 5b) depended on a three-way interactive effect of temperature,  $pCO_2$  and time of  
 454 measurement (interactive effect Time  $\times$  T  $\times pCO_2$ ;  $F_{1,28} = 4.64$ ,  $p = 0.040$ ). Daytime  $G_{TA}$  rates  
 455 were positive across treatments but declined to negative values under dark conditions in all  
 456 except the control treatments. During daytime  $G_{TA}$  rates were unaffected by levels of temperature  
 457 and  $pCO_2$ , while elevated  $pCO_2$  decreased  $G_{TA}$  rates at nighttime irrespective of temperature  
 458 (Tukey HSD  $p = 0.018$ ).



459  
 460 **Figure 5.** End-of-treatment day and night-time calcification rates ( $G_{TA}$ ; mean  $\pm$  SE) under  
 461 different treatments of warming and acidification for *Acropora intermedia* (a) and *Porites lobata*  
 462 (b). Rates ( $n = 8$  per treatment) were measured after seven weeks of exposure to independent and  
 463 concurrent levels of temperature and  $pCO_2$  according to end-of-century RCP8.5 projections. The  
 464 blue text inside the panels indicates the presence of significant 3-way interactive effects of time  
 465 (day/night), warming and acidification (3-inter).

466

## 467 **Discussion**

468 The present study assessed the two global stressors most commonly associated with future  
469 emission scenarios, namely elevated temperature and  $p\text{CO}_2$ . We did so under an experimental  
470 design that preserved the natural diel and seasonal fluctuations in temperature and  $p\text{CO}_2$  by  
471 superimposing future conditions on a present-day baseline. This allowed full interaction of  
472 environmental drivers under their naturally variable ranges, and produces accurate organismal  
473 responses to their environment. The present study reveals that tropical symbiotic corals  
474 experience physiological impairment, extensive bleaching and mortality when exposed to end-  
475 of-century, non-El Niño summer thermal and OA regimes under RCP8.5 scenarios (570 ppm  
476  $p\text{CO}_2$  and 3.5 °C above PD values). Thermal stress was identified as the main driver of  
477 physiological changes and mortality due to its correlation with coral bleaching. Collapse of  
478 primary productivity, stored energy reserves and skeleton accretion were the main drivers of  
479 observed mortality. These effects were evident in both species, though the decline was stronger  
480 in *A. intermedia* compared to *P. lobata*.

481

### 482 *Thermal stress and bleaching*

483 The RCP8.5 emissions scenario implies far more challenging thermal conditions than expected  
484 under the 2015 Paris Agreement, which aims to stabilize average global temperatures below 2 °C  
485 above preindustrial values (Hoegh-Guldberg et al., 2019). Emission rates currently follow the  
486 RCP8.5 pathway projections (Jackson et al., 2017; Le Quéré et al., 2018), and future reefs will  
487 likely experience annual heat waves exceeding present-day extremes (Frieler et al., 2013; van  
488 Hoodonk et al., 2016). Even before projected end-of-century conditions will be reached,  
489 summer bleaching and El Niño events will likely increase in frequency (Cai et al., 2014). The  
490 2016 and 2017 bleaching events were the worst in GBR history, with >60% bleaching in the  
491 northern regions (Hughes et al., 2017), followed by significant subsequent mortality. During  
492 these bleaching events, northern GBR reefs experienced >4 (high likelihood for severe coral  
493 bleaching) and >8 (high likelihood for widespread coral mortality) °C weeks over approximately  
494 four and three months respectively, and peaking at approximately 15.5 °C weeks (NOAA CRF 5

495 km satellite data; Hughes et al., 2019). Thermal conditions in the high temperature treatment of  
496 the present study - which preceded the 2016-2017 bleaching events - exceeded 4 °C weeks for  
497 more than five weeks and 8 °C weeks for three weeks, before peaking at 15.6 °C weeks at the  
498 termination of the experiment in mid-February, approximately when annual thermal peaks are  
499 typically attained in this region of the GBR (NOAA virtual stations, 5km). By then, both *A.*  
500 *intermedia* and *P. lobata* had bleached severely and *A. intermedia* mortality had reached 50%, a  
501 proportion that would have likely increased further under extended periods of DHW >8, had the  
502 experiment been continued to the end of summer.

503

#### 504 *Treatment effects on growth, productivity and energy reserves*

505 Long-term averages of skeleton accretion ( $G_{DW}$ ) as well as increases in skeleton volume for both  
506 *A. intermedia* and *P. lobata* (Fig. 4) declined concurrently, although they remained positive.  
507 However, in *A. intermedia* these changes were primarily temperature driven compared to  $pCO_2$   
508 driven in *P. lobata*. The concurrent decrease in skeleton  $G_{DW}$  and volume suggests no shift  
509 between skeleton extension and bulk density, contrasting previous studies showing deteriorating  
510 skeleton density and structure under OA (Crook, Cohen, Rebolledo-Vieyra, Hernandez, &  
511 Paytan, 2013; Fantazzini et al., 2015; Tambutté et al., 2015). However, analysis of end-of-  
512 treatment rates of calcification (Fig. 5) revealed a negative effect of  $pCO_2$  on skeletogenesis in  
513 both species, ultimately resulting in net skeleton dissolution in *A. intermedia*. However, this was  
514 only the case under dark conditions or otherwise absence of photosynthetic activity (i.e.  
515 bleaching), as demonstrated by the collapse of calcification in *A. intermedia* under thermal stress.  
516 Our results demonstrate the importance of photosynthetic activity to calcification, particularly in  
517 *A. intermedia*. The ability to maintain photosynthesis during daytime greatly mitigated the  
518 negative effects of acidification on  $G_{TA}$  through internal pH upregulation and energy supply  
519 (Dufault et al., 2013; McCulloch, Falter, Trotter, & Montagna, 2012; Wall et al., 2016), despite  
520 growing in a seawater  $\Omega_{ARAG}$  of approximately 2.3. Effects of elevated  $pCO_2$  were strong under  
521 night-time conditions, owing to a reduction in seawater pH which was exacerbated by additional  
522 respiration and deficiency of photosynthetic products at the calciblastic layer (Colombo-  
523 Pallotta, Rodríguez-Román, & Iglesias-Prieto, 2010; Venn et al., 2013). In bleached *A.*  
524 *intermedia*  $G_{TA}$  was negative, despite average seawater  $\Omega_{ARAG}$  values of 3.39 (Table 1) and

525 daytime  $G_{TA}$  was not reduced in either species as long as photosynthetic rates were maintained  
526 (Levas, Grottoli, Hughes, Osburn, & Matsui, 2013). The constraints of elevated temperature and  
527 acidification on long and short-term measures of skeleton growth will, provided that corals  
528 survive, limit reef capacity to outpace sea-level rise and decrease resilience to extreme weather  
529 (Manzello et al., 2008; Mollica et al., 2018; van Woesik, Golbuu, & Roff, 2015).

530 Elevated  $pCO_2$  reduced  $R_{DARK}$  and  $P_{NET}$  in *A. intermedia* but not in *P. lobata*. The effect of  
531 seawater acidification on coral photosynthesis is uncertain, with previous studies observing  
532 either small or no changes of photosynthesis under lower pH (Anthony, Kline, Diaz-Pulido,  
533 Dove, & Hoegh-Guldberg, 2008; Comeau, Carpenter, & Edmunds, 2016; Hoadley et al., 2015;  
534 Marubini, Ferrier-Pagès, Furla, & Allemand, 2008). Reduction of the symbiont population  
535 density under heat stress in both species of this study was similar and unaffected by elevated  
536  $pCO_2$ , consistent with the hypothesis that temperature is the dominant bleaching agent (Hughes  
537 et al., 2017; Schoepf et al., 2013, 2019). However,  $P_{NET}$  did not decline equally in the two  
538 species. In *A. intermedia*  $P_{NET}$  decreased proportionally to symbiont loss, whereas in *P. lobata*  
539  $P_{NET}$  only dropped by 50% after a 95% symbiont decline. This could indicate a high degree of  
540 self-shading in endosymbionts present in unbleached *P. lobata* (Enríquez, Méndez, & Iglesias-  
541 Prieto, 2005; Hoogenboom, Connolly, & Anthony, 2008), or lower susceptibility of  
542 photosynthesis to heat stress in thermally tolerant *Cladocopium* C15 in massive *Porites* (Fisher,  
543 Malme, & Dove, 2012). Alternatively,  $P_{NET}$  could be compensated by a significant endolithic  
544 algae community typical of *Porites* sp. (Marcelino, Morrow, van Oppen, Bourne, & Verbruggen,  
545 2017; Shashar, Banaszak, Lesser, & Amrami, 1997). Endolithic algae are known to increase in  
546 abundance in stressed corals, though it remains unclear why (Fine & Loya, 2002; Reyes-Nivia,  
547 Diaz-Pulido, Kline, Guldberg, & Dove, 2013). We observed a 3 mm thick green band underlying  
548 the coral tissue in *P. lobata*, approximately 5 mm into the skeleton, indicating that endolithic  
549 algae photosynthesis may have been responsible for the compensation in  $P_{NET}$  after symbiont  
550 loss. Retaining photosynthetic rates and a supply of photosynthates from endolithic algae partly  
551 mitigates the detrimental effects of heat stress and bleaching (Fine & Loya, 2002), and may help  
552 corals to sustain the theoretical autotrophic break-even point at  $P_{NET}:R_{DARK} = 1$  (Muscatine,  
553 McCloskey, & Marian, 1981). In the present study, bleached *P. lobata* were able to maintain a  
554  $P_{NET}:R_{DARK}$  ratio of approximately 1, while this ratio was nearly zero in bleached *A. intermedia*.  
555 This suggests that *P. lobata* may still be receiving some autotrophic carbon to maintain basic

556 metabolic functions even when bleached, while *A. intermedia* would have to switch to  
557 heterotrophy or stored energy reserves for metabolism (Grottoli, Rodrigues, & Palardy, 2006;  
558 Rodrigues & Grottoli, 2007). Additionally, high heterotrophic capacity and somatic energy  
559 reserves in *P. lobata* compared to *A. intermedia* likely benefit this species during bleaching  
560 (Levas, Grottoli, Hughes, Osburn, & Matsui, 2013; Palardy, Rodrigues, & Grottoli, 2008).

561 Heterotrophic compensation for photosynthetic losses could alleviate immediate energetic stress  
562 after bleaching (Baumann, Grottoli, Hughes, & Matsui, 2014; Grottoli, Rodrigues, & Palardy,  
563 2006; Hughes, Grottoli, Pease, & Matsui, 2010), and possibly aid recovery (Levas, Grottoli,  
564 Hughes, Osburn, & Matsui, 2013). However, this is possibly insufficient for survival when corals  
565 remain bleached over longer timescales (Anthony, Connolly, & Hoegh-Guldberg, 2007;  
566 Anthony, Hoogenboom, Maynard, Grottoli, & Middlebrook, 2009; Grottoli et al., 2006).  
567 Previous studies have demonstrated enhanced heterotrophic feeding capacity in selective coral  
568 species under thermal stress (Ferrier-Pagès, Rottier, Beraud, & Levy, 2010; Grottoli et al., 2014;  
569 Grottoli, Rodrigues, & Palardy, 2006; Hughes, Grottoli, Pease, & Matsui, 2010), and  
570 improvement of coral thermal tolerance through heterotrophy-derived nutrients (Ferrier-Pagès,  
571 Sauzéat, & Balter, 2018). In the present experiment, corals were fed thawed *Artemia* at  
572 concentrations similar to those of ambient zooplankton *in situ*, since the 10 µm filter of our  
573 water inlet had removed most larger prey normally contributing to the coral diet (Houlbrèque &  
574 Ferrier-Pagès, 2009; Palardy, Grottoli, & Matthews, 2005). Visual inspection confirmed tentacle  
575 extension and feeding behavior in both bleached and unbleached living corals, indicating that  
576 feeding capacity was not affected by RCP8.5 scenario conditions. However, the decline in host  
577 tissue protein and lipid concentrations under thermal stress indicates at least a partial failure of  
578 heterotrophy to compensate for loss in photosynthates (Hughes et al., 2010).

579 Lipid and protein concentrations in unbleached specimens of both species were comparable to  
580 concentrations found for healthy corals of similar genera in previous studies (Hoogenboom,  
581 Rottier, Sikorski, & Ferrier-Pagès, 2015) but declined markedly under thermal stress, particularly  
582 in *A. intermedia*. Lipid catabolism by bleached corals additionally fulfils immediate metabolic  
583 demands in the absence of photosynthetic carbon (Fitt, Spero, Halas, White, & Porter, 1993;  
584 Grottoli, Rodrigues, & Juarez, 2004; Grottoli & Rodrigues, 2011). However, the exhaustion of  
585 stored energy reserves has been linked to rapid increases in mortality of coral larvae (Graham,



586 Baird, Connolly, Sewell, & Willis, 2017) and adult colonies (Anthony, Connolly, & Hoegh-  
587 Guldberg, 2007; Bay, Guérécheau, Andreakis, Ulstrup, & Matz, 2013; Kenkel, Meyer, & Matz,  
588 2013). We observed a significant increase in *A. intermedia* mortality when thermally stressed,  
589 concomitant with diminished tissue protein and lipid concentrations. *P. lobata* mortality  
590 remained low (10%), despite significant declines in tissue lipid and protein concentrations under  
591 thermal stress. The present study ended in mid-February, before the end of the annual thermal  
592 maximum period on Heron Island. Previous studies have described a lagging effect between  
593 thermal stress and physiological decline in several coral species including *P. lobata* (Levas,  
594 Grottoli, Hughes, Osburn, & Matsui, 2013; Rodrigues & Grottoli, 2007), thus energetic  
595 exhaustion and mortality in our study could be worsened over the full duration of summer  
596 (Hughes et al., 2017).

597

598 *Not all corals are equal*

599 *A. intermedia* and *P. lobata* clearly respond differently to elevated temperature and acidification.  
600 Bleaching in *A. intermedia* started approximately 5 weeks earlier than in *P. lobata*, and *A.*  
601 *intermedia* mortality was significant under elevated temperature. Furthermore, the collapse of  
602 day and nighttime  $G_{TA}$  and productivity in *A. intermedia* was more severe than in *P. lobata*, but  
603 acidification affected night-time  $G_{TA}$  more in *P. lobata*. Coral species are known to differ in their  
604 sensitivity to environmental cues (Fabricius et al., 2011), determined by a combination of factors  
605 such as host identity (Fitt et al., 2009; Hoadley et al., 2019), Symbiodiniaceae type(s) hosted (Fitt  
606 et al., 2009; Sampayo, Ridgway, Bongaerts, & Hoegh-Guldberg, 2008) and nearby benthic  
607 community composition (Dove et al., 2013). At Heron Island *A. intermedia* has been found to  
608 harbor thermally sensitive *Cladocopium* C3, while *P. lobata* harbored predominantly thermally  
609 tolerant *Cladocopium* C15 (Fisher, Malme, & Dove, 2012; LaJeunesse et al., 2004), likely  
610 explaining the later onset of bleaching in *P. lobata*. The introduction of symbiont-specific traits  
611 and other varying factors may lead to trade-offs in coral performance (Jones & Berkelmans,  
612 2011), and invites further experiments studying different combinations of environments and  
613 organisms to discern future climate impacts on reef health and survival (Bay, Rose, Logan, &  
614 Palumbi, 2017; Hoadley et al., 2019; Wall, Mason, Ellis, Cunning, & Gates, 2017). Our results  
615 show that *P. lobata* is more tolerant to thermal and OA stress than *A. intermedia*. Although

616 warming is the dominant driver of holobiont response in both species (Fig. 2), temperature  
617 impacts fundamental physiological and metabolic properties more strongly in *A. intermedia*.  
618 Aside from some exceptions (Kim et al., 2019), this is in accordance with findings from previous  
619 research that classify *Porites* sp. as temperature tolerant and *Acropora* sp. as temperature  
620 sensitive (Fabricius et al., 2011; Loya et al., 2001; Marshall & Baird, 2000), though this may  
621 shift as global warming intensifies (Grottoli et al., 2014; Rodolfo-Metalpa et al., 2014).

622

### 623 *Concluding remarks*

624 Changes in metabolism and physiology in both coral species under elevated temperature and  
625 acidification were invariably negative, and mostly driven by heat stress. Previous studies  
626 reported mixed, and often interactive effects (Bahr, Jokiel, & Rodgers, 2016; Büscher, Form, &  
627 Riebesell, 2017; Edmunds, Brown, & Moriarty, 2012; Reynaud et al., 2003; Schoepf et al.,  
628 2013), but these were under more moderate temperature and acidification conditions than the  
629 end-of-century conditions of the RCP8.5 scenario, and not during peak summer conditions.  
630 There was no evidence of synergistic behavior of thermal and acidification effects in this study.  
631 Our results demonstrate that under extreme, end-of-century summer conditions of the business-  
632 as-usual emissions scenario coral bleaching becomes inevitable even in heat-tolerant species, and  
633 furthermore suggest that the ensuing prolonged collapse of photosynthesis dominates all other  
634 processes (Anthony, Connolly, & Hoegh-Guldberg, 2007; Grottoli, Rodrigues, & Juarez, 2004).  
635 Additionally, the interaction of natural diel  $p\text{CO}_2$  fluctuations with benthic community  
636 metabolism and decreased seawater buffer capacity under future conditions likely drives a severe  
637 widening of the  $\text{CO}_2$  range that reefs will be exposed to in the future compared to that predicted  
638 by atmospheric models (Shaw, McNeil, Tilbrook, Matear, & Bates, 2013), exerting additional  
639 stress on these ecosystems.

640 Worldwide, coral health and growth have already significantly decreased over the last decades,  
641 often as a result of climate change (Baumann et al., 2019; Cantin, Cohen, Karnauskas, Tarrant, &  
642 McCorkle, 2010; Cooper, De'ath, Fabricius, & Lough, 2008; Mellin et al., 2019; Perry et al.,  
643 2015). Our study indicates that this pattern will become increasingly problematic in the future as  
644 conditions worsen (Lough, Anderson, & Hughes, 2018; van Hooidonk et al., 2016), unless corals  
645 are able to adapt rapidly. The acclimation or adaptation capacity of symbiotic corals to

646 environmental change is uncertain, (Berkelmans & van Oppen, 2006; Pandolfi, Connolly,  
647 Marshall, & Cohen, 2011; Sully, Burkepile, Donovan, Hodgson, & van Woesik, 2019; Wright et  
648 al., 2019), and differs between species (Grottoli et al., 2014). The finding that some present-day  
649 corals fare better under conditions of a century ago suggests that little adaptation has occurred so  
650 far (Dove et al., 2013). Meanwhile, some species are close to their upper limit in short-term  
651 thermal acclimation (Schoepf et al., 2019), and may not be able to keep pace under the rapidly  
652 increasing temperature conditions of the RCP8.5 scenario (Bay, Rose, Logan, & Palumbi, 2017;  
653 Hoegh-Guldberg, 2012). Thermally sensitive groups (e.g. Acroporids) have been severely  
654 impacted by warming in recent years (Kim et al., 2019; Le Nohaïc et al., 2017) and are already  
655 facing local extinction (Riegl et al., 2018). Recurring thermal anomalies predicted under RCP8.5  
656 emission pathways will likely cause the disappearance of thermally-sensitive coral species from  
657 reefs globally before 2100 (Lough, Anderson, & Hughes, 2018), while annually recurring  
658 bleaching could prove devastating to even some of the most thermally-tolerant species (Grottoli  
659 et al., 2014). Overall, if warming continues unabated, future reefs will be severely reduced in  
660 diversity and populated by only the most resilient coral species.

661

## 662 **Acknowledgements**

663 This research was funded by the NOAA Coral Reef Watch and the Australian Research Council  
664 (ARC), the ARC Centre of Excellence for Coral Reef Studies grant CE0561435 and ARC  
665 Laureate grant FL120100066 (to OHG and SD), a University of Queensland International  
666 Scholarship UQI and a Holsworth Wildlife Research Endowment (Equity Trustees Charitable  
667 Foundation) grant (to RZ). We thank Aaron Chai, Giovanni Bernal-Carrillo, Annamieke van den  
668 Heuvel and Mark Snowball for support and assistance with the T/CO<sub>2</sub> system, as well as Stijn  
669 den Haan, Christopher Brunner and the HIRS staff for their help in the field. Sample collection  
670 and experimental work occurred under permit G14/37212.1 issued by the GBR Marine Park  
671 Authority.

672

673 Author contributions

674 RZ, SD and OHG conceived and designed the study. RZ and MA performed the experiment.  
675 Data were analyzed by RZ, SD and MA, and DB, AK and OHG contributed to data  
676 interpretation. RZ wrote the manuscript with all co-authors contributing to its final form.

677

#### 678 **Data sharing and accessibility**

679 The data that support the findings of this study are available from the corresponding author upon  
680 reasonable request.

681

#### 682 **References**

683 Achlatis, M., van der Zande, R. M., Schönberg, C. H. L., Fang, J. K. H., Hoegh-Guldberg, O., &  
684 Dove, S. (2017). Sponge bioerosion on changing reefs: ocean warming poses physiological  
685 constraints to the success of a photosymbiotic excavating sponge. *Scientific Reports*, 7(1),  
686 10705. <https://doi.org/10.1038/s41598-017-10947-1>

687 Anthony, K. R. N., Connolly, S. R., & Hoegh-Guldberg, O. (2007). Bleaching, energetics, and  
688 coral mortality risk: Effects of temperature, light, and sediment regime. *Limnology and*  
689 *Oceanography*, 52(2), 716–726. <https://doi.org/10.4319/lo.2007.52.2.0716>

690 Anthony, K. R. N., Hoogenboom, M. O., Maynard, J. A., Grottoli, A. G., & Middlebrook, R.  
691 (2009). Energetics approach to predicting mortality risk from environmental stress: a case  
692 study of coral bleaching. *Functional Ecology*, 23(3), 539–550. [https://doi.org/10.1111/j.1365-](https://doi.org/10.1111/j.1365-2435.2008.01531.x)  
693 [2435.2008.01531.x](https://doi.org/10.1111/j.1365-2435.2008.01531.x)

694 Anthony, K. R. N., Kline, D. I., Diaz-Pulido, G., Dove, S., & Hoegh-Guldberg, O. (2008). Ocean  
695 acidification causes bleaching and productivity loss in coral reef builders. *Proceedings of the*  
696 *National Academy of Sciences of the United States of America*, 105(45), 17442–6.  
697 <https://doi.org/10.1073/pnas.0804478105>

698 Bahr, K. D., Jokiel, P. L., & Rodgers, K. S. (2016). Seasonal and annual calcification rates of the  
699 Hawaiian reef coral, *Montipora capitata*, under present and future climate change scenarios.  
700 *ICES Journal of Marine Science*, 74(4), 1083–1091. <https://doi.org/10.1093/icesjms/fsw078>

- 701 Baumann, J., Grottoli, A. G., Hughes, A. D., & Matsui, Y. (2014). Photoautotrophic and  
702 heterotrophic carbon in bleached and non-bleached coral lipid acquisition and storage.  
703 *Journal of Experimental Marine Biology and Ecology*, 461, 469–478.  
704 <https://doi.org/10.1016/j.jembe.2014.09.017>
- 705 Baumann, J. H., Ries, J. B., Rippe, J. P., Courtney, T. A., Aichelman, H. E., Westfield, I., &  
706 Castillo, K. D. (2019). Nearshore coral growth declining on the Mesoamerican Barrier Reef  
707 System. *Global Change Biology*, 25(11), 3932–3945. <https://doi.org/10.1111/gcb.14784>
- 708 Bay, L. K., Guérécheau, A., Andreakis, N., Ulstrup, K. E., & Matz, M. V. (2013). Gene  
709 expression signatures of energetic acclimatisation in the reef building coral *Acropora*  
710 *millepora*. *PLoS ONE*, 8(5), e61736. <https://doi.org/10.1371/journal.pone.0061736>
- 711 Bay, R. A., Rose, N. H., Logan, C. A., & Palumbi, S. R. (2017). Genomic models predict  
712 successful coral adaptation if future ocean warming rates are reduced. *Science Advances*,  
713 3(11), e1701413. <https://doi.org/10.1126/sciadv.1701413>
- 714 Berkelmans, R. (2002). Time-integrated thermal bleaching thresholds of reefs and their variation  
715 on the Great Barrier Reef. *Marine Ecology Progress Series*, 229, 73-82.  
716 <https://doi.org/10.2307/24865053>
- 717 Berkelmans, R., & van Oppen, M. J. . (2006). The role of zooxanthellae in the thermal tolerance  
718 of corals: a “nugget of hope” for coral reefs in an era of climate change. *Proceedings of the*  
719 *Royal Society B: Biological Sciences*, 273(1599), 2305–2312.  
720 <https://doi.org/10.1098/rspb.2006.3567>
- 721 Büscher, J. V., Form, A. U., & Riebesell, U. (2017). Interactive effects of ocean acidification and  
722 warming on growth, fitness and survival of the cold-water coral *Lophelia pertusa* under  
723 different food availabilities. *Frontiers in Marine Science*, 4.  
724 <https://doi.org/10.3389/fmars.2017.00101>
- 725 Cai, W., Borlace, S., Lengaigne, M., van Rensch, P., Collins, M., Vecchi, G., ... Jin, F.-F.  
726 (2014). Increasing frequency of extreme El Niño events due to greenhouse warming. *Nature*  
727 *Climate Change*, 4(2), 111–116. <https://doi.org/10.1038/nclimate2100>
- 728 Cantin, N. E., Cohen, A. L., Karnauskas, K. B., Tarrant, A. M., & McCorkle, D. C. (2010).

- 729 Ocean warming slows coral growth in the central Red Sea. *Science*, 329(5989).  
730 <https://doi.org/10.1126/science.1190182>
- 731 Chan, W. Y., & Eggins, S. M. (2017). Calcification responses to diurnal variation in seawater  
732 carbonate chemistry by the coral *Acropora formosa*. *Coral Reefs*, 36(3), 763–772.  
733 <https://doi.org/10.1007/s00338-017-1567-8>
- 734 Chisholm, J. R. M., & Gattuso, J.-P. (1991). Validation of the alkalinity anomaly technique for  
735 investigating calcification of photosynthesis in coral reef communities. *Limnology and*  
736 *Oceanography*, 36(6), 1232–1239. <https://doi.org/10.4319/lo.1991.36.6.1232>
- 737 Cohen, A. L., McCorkle, D. C., de Putron, S., Gaetani, G. A., & Rose, K. A. (2009).  
738 Morphological and compositional changes in the skeletons of new coral recruits reared in  
739 acidified seawater: Insights into the biomineralization response to ocean acidification.  
740 *Geochemistry, Geophysics, Geosystems*, 10(7). <https://doi.org/10.1029/2009GC002411>
- 741 Colombo-Pallotta, M. F., Rodríguez-Román, A., & Iglesias-Prieto, R. (2010). Calcification in  
742 bleached and unbleached *Montastraea faveolata*: evaluating the role of oxygen and glycerol.  
743 *Coral Reefs*, 29(4), 899–907. <https://doi.org/10.1007/s00338-010-0638-x>
- 744 Comeau, S., Carpenter, R. C., & Edmunds, P. J. (2016). Effects of  $p\text{CO}_2$  on photosynthesis and  
745 respiration of tropical scleractinian corals and calcified algae. *ICES Journal of Marine*  
746 *Science*, 74(4), 1092–1102. <https://doi.org/10.1093/icesjms/fsv267>
- 747 Comeau, S., Edmunds, P., Spindel, N., & Carpenter, R. (2014). Diel  $p\text{CO}_2$  oscillations modulate  
748 the response of the coral *Acropora hyacinthus* to ocean acidification. *Marine Ecology*  
749 *Progress Series*, 501, 99–111. <https://doi.org/10.3354/meps10690>
- 750 Cooper, T., De'ath, G., Fabricius, K. E., & Lough, J. M. (2008). Declining coral calcification in  
751 massive *Porites* in two nearshore regions of the northern Great Barrier Reef. *Global Change*  
752 *Biology*, 14(3), 529–538. <https://doi.org/10.1111/j.1365-2486.2007.01520.x>
- 753 Courtney, T. A., Lebrato, M., Bates, N. R., Collins, A., de Putron, S. J., Garley, R., ...  
754 Andersson, A. J. (2017). Environmental controls on modern scleractinian coral and reef-scale  
755 calcification. *Science Advances*, 3(11), e1701356. <https://doi.org/10.1126/sciadv.1701356>
- 756 Crook, E. D., Cohen, A. L., Rebolledo-Vieyra, M., Hernandez, L., & Paytan, A. (2013). Reduced

757 calcification and lack of acclimatization by coral colonies growing in areas of persistent  
758 natural acidification. *Proceedings of the National Academy of Sciences of the United States of*  
759 *America*, 110(27), 11044–9. <https://doi.org/10.1073/pnas.1301589110>

760 Darling, E. S., Alvarez-Filip, L., Oliver, T. A., McClanahan, T. R., & Côté, I. M. (2012).  
761 Evaluating life-history strategies of reef corals from species traits. *Ecology Letters*, 15(12),  
762 1378–1386. <https://doi.org/10.1111/j.1461-0248.2012.01861.x>

763 Darling, E. S., McClanahan, T. R., & Côté, I. M. (2013). Life histories predict coral community  
764 disassembly under multiple stressors. *Global Change Biology*, 19(6), 1930–1940.  
765 <https://doi.org/10.1111/gcb.12191>

766 Dickson, A. G., Afghan, J. D., & Anderson, G. C. (2003). Reference materials for oceanic CO<sub>2</sub>  
767 analysis: a method for the certification of total alkalinity. *Marine Chemistry*, 80(2–3), 185–  
768 197. [https://doi.org/10.1016/S0304-4203\(02\)00133-0](https://doi.org/10.1016/S0304-4203(02)00133-0)

769 Dove, S. G., Kline, D. I., Pantos, O., Angly, F. E., Tyson, G. W., & Hoegh-Guldberg, O. (2013).  
770 Future reef decalcification under a business-as-usual CO<sub>2</sub> emission scenario. *Proceedings of*  
771 *the National Academy of Sciences of the United States of America*, 110(38), 15342–7.  
772 <https://doi.org/10.1073/pnas.1302701110>

773 Drenkard, E. J., Cohen, A. L., McCorkle, D. C., de Putron, S. J., Starczak, V. R., & Zicht, A. E.  
774 (2013). Calcification by juvenile corals under heterotrophy and elevated CO<sub>2</sub>. *Coral Reefs*,  
775 32(3), 727–735. <https://doi.org/10.1007/s00338-013-1021-5>

776 Dufault, A. M., Ninokawa, A., Bramanti, L., Cumbo, V. R., Fan, T.-Y., & Edmunds, P. J. (2013).  
777 The role of light in mediating the effects of ocean acidification on coral calcification. *The*  
778 *Journal of Experimental Biology*, 216, 1570–1577. <https://doi.org/10.1242/jeb.080549>

779 Dunn, S. R., Thomas, M. C., Nette, G. W., Dove, S. G., & Blackburn, S. (2012). A lipidomic  
780 approach to understanding free fatty acid lipogenesis derived from dissolved inorganic carbon  
781 within Cnidarian-Dinoflagellate symbiosis. *PLoS ONE*, 7(10), e46801.  
782 <https://doi.org/10.1371/journal.pone.0046801>

783 Edmunds, P. J., Brown, D., & Moriarty, V. (2012). Interactive effects of ocean acidification and  
784 temperature on two scleractinian corals from Moorea, French Polynesia. *Global Change*

785 *Biology*, 18(7), 2173–2183. <https://doi.org/10.1111/j.1365-2486.2012.02695.x>

786 Enríquez, S., Méndez, E. R., & Iglesias-Prieto, R. (2005). Multiple scattering on coral skeletons  
787 enhances light absorption by symbiotic algae. *Limnology and Oceanography*, 50(4), 1025–  
788 1032. <https://doi.org/10.4319/lo.2005.50.4.1025>

789 Fabricius, K. E., Langdon, C., Uthicke, S., Humphrey, C., Noonan, S., De'ath, G., ... Lough, J.  
790 M. (2011). Losers and winners in coral reefs acclimatized to elevated carbon dioxide  
791 concentrations. *Nature Climate Change*, 1(3), 165–169. <https://doi.org/10.1038/nclimate1122>

792 Fantazzini, P., Mengoli, S., Pasquini, L., Bortolotti, V., Brizi, L., Mariani, M., ... Goffredo, S.  
793 (2015). Gains and losses of coral skeletal porosity changes with ocean acidification  
794 acclimation. *Nature Communications*, 6(1), 7785. <https://doi.org/10.1038/ncomms8785>

795 Ferrier-Pagès, C., Rottier, C., Beraud, E., & Levy, O. (2010). Experimental assessment of the  
796 feeding effort of three scleractinian coral species during a thermal stress: Effect on the rates of  
797 photosynthesis. *Journal of Experimental Marine Biology and Ecology*, 390(2), 118–124.  
798 <https://doi.org/10.1016/J.JEMBE.2010.05.007>

799 Ferrier-Pagès, C., Sauzéat, L., & Balter, V. (2018). Coral bleaching is linked to the capacity of  
800 the animal host to supply essential metals to the symbionts. *Global Change Biology*, 24(7),  
801 3145–3157. <https://doi.org/10.1111/gcb.14141>

802 Fine, M., & Loya, Y. (2002). Endolithic algae: an alternative source of photoassimilates during  
803 coral bleaching. *Proceedings of the Royal Society of London B: Biological Sciences*,  
804 269(1497), 1205–1210. <https://doi.org/10.1098/rspb.2002.1983>

805 Fisher, P. L., Malme, M. K., & Dove, S. (2012). The effect of temperature stress on coral–  
806 *Symbiodinium* associations containing distinct symbiont types. *Coral Reefs*, 31(2), 473–485.  
807 <https://doi.org/10.1007/s00338-011-0853-0>

808 Fitt, W. K., Gates, R. D., Hoegh-Guldberg, O., Bythell, J. C., Jatkar, A., Grottoli, A. G., ...  
809 Lesser, M. P. (2009). Response of two species of Indo-Pacific corals, *Porites cylindrica* and  
810 *Stylophora pistillata*, to short-term thermal stress: The host does matter in determining the  
811 tolerance of corals to bleaching. *Journal of Experimental Marine Biology and Ecology*,  
812 373(2), 102–110. <https://doi.org/10.1016/j.jembe.2009.03.011>



- 813 Fitt, W. K., Spero, H. J., Halas, J., White, M. W., & Porter, J. W. (1993). Recovery of the coral  
814 *Montastrea annularis* in the Florida Keys after the 1987 Caribbean “bleaching event.” *Coral*  
815 *Reefs*, 12(2), 57–64. <https://doi.org/10.1007/BF00302102>
- 816 Frieler, K., Meinshausen, M., Golly, A., Mengel, M., Lebek, K., Donner, S. D., & Hoegh-  
817 Guldberg, O. (2013). Limiting global warming to 2 °C is unlikely to save most coral reefs.  
818 *Nature Climate Change*, 3(2), 165–170. <https://doi.org/10.1038/nclimate1674>
- 819 Gaffey, S. J., & Bronnimann, C. E. (1993). Effects of bleaching on organic and mineral phases in  
820 biogenic carbonates. *Journal of Sedimentary Research*, 63(4), 752–754.  
821 <https://doi.org/10.1306/D4267BE0-2B26-11D7-8648000102C1865D>
- 822 Godinot, C., Houlbrèque, F., Grover, R., Ferrier-Pagès, C., & Larsen, A. (2011). Coral uptake of  
823 inorganic phosphorus and nitrogen negatively affected by simultaneous changes in  
824 temperature and pH. *PLoS ONE*, 6(9), e25024. <https://doi.org/10.1371/journal.pone.0025024>
- 825 Graham, E. M., Baird, A. H., Connolly, S. R., Sewell, M. A., & Willis, B. L. (2017). Uncoupling  
826 temperature-dependent mortality from lipid depletion for scleractinian coral larvae. *Coral*  
827 *Reefs*, 36(1), 97–104. <https://doi.org/10.1007/s00338-016-1501-5>
- 828 Grottoli, A. G., & Rodrigues, L. J. (2011). Bleached *Porites compressa* and *Montipora capitata*  
829 corals catabolize  $\delta^{13}\text{C}$ -enriched lipids. *Coral Reefs*, 30(3), 687.  
830 <https://doi.org/10.1007/s00338-011-0756-0>
- 831 Grottoli, A. G., Rodrigues, L. J., & Juarez, C. (2004). Lipids and stable carbon isotopes in two  
832 species of Hawaiian corals, *Porites compressa* and *Montipora verrucosa*, following a  
833 bleaching event. *Marine Biology*, 145(3), 621–631. [https://doi.org/10.1007/s00227-004-1337-](https://doi.org/10.1007/s00227-004-1337-3)  
834 3
- 835 Grottoli, A. G., Rodrigues, L. J., & Palardy, J. E. (2006). Heterotrophic plasticity and resilience  
836 in bleached corals. *Nature*, 440(7088), 1186–1189. <https://doi.org/10.1038/nature04565>
- 837 Grottoli, A. G., Warner, M. E., Levas, S. J., Aschaffenburg, M. D., Schoepf, V., McGinley, M.,  
838 ... Matsui, Y. (2014). The cumulative impact of annual coral bleaching can turn some coral  
839 species winners into losers. *Global Change Biology*, 20(12), 3823–3833.  
840 <https://doi.org/10.1111/gcb.12658>

- 841 Guest, J. R., Low, J., Tun, K., Wilson, B., Ng, C., Raingeard, D., ... Steinberg, P. D. (2016).  
842 Coral community response to bleaching on a highly disturbed reef. *Scientific Reports*, 6(1),  
843 20717. <https://doi.org/10.1038/srep20717>
- 844 Hoadley, K. D., Lewis, A. M., Wham, D. C., Pettay, D. T., Grasso, C., Smith, R., ... Warner, M.  
845 E. (2019). Host–symbiont combinations dictate the photo-physiological response of reef-  
846 building corals to thermal stress. *Scientific Reports*, 9(1), 9985.  
847 <https://doi.org/10.1038/s41598-019-46412-4>
- 848 Hoadley, K. D., Pettay, D. T., Grottoli, A. G., Cai, W.-J., Melman, T. F., Schoepf, V., ...  
849 Warner, M. E. (2015). Physiological response to elevated temperature and  $p\text{CO}_2$  varies across  
850 four Pacific coral species: Understanding the unique host+symbiont response. *Scientific*  
851 *Reports*, 5, 18371. <https://doi.org/10.1038/srep18371>
- 852 Hoadley, K. D., Pettay, D. T., Grottoli, A. G., Cai, W. J., Melman, T. F., Levas, S., ... Warner,  
853 M. E. (2016). High-temperature acclimation strategies within the thermally tolerant  
854 endosymbiont *Symbiodinium trenchii* and its coral host, *Turbinaria reniformis*, differ with  
855 changing  $p\text{CO}_2$  and nutrients. *Marine Biology*, 163(6), 1–13. [https://doi.org/10.1007/s00227-](https://doi.org/10.1007/s00227-016-2909-8)  
856 [016-2909-8](https://doi.org/10.1007/s00227-016-2909-8)
- 857 Hoegh-Guldberg, O. (2012). The adaptation of coral reefs to climate change: Is the Red Queen  
858 being outpaced? *Scientia Marina*, 76(2), 403–408. <https://doi.org/10.3989/scimar.03660.29A>
- 859 Hoegh-Guldberg, O., Cai, R., Poloczanska, E. S. S., Brewer, P. G. G., Sundby, S., Hilmi, K., ...  
860 Jung, S. (2014). The Ocean. In C. U. Press (Ed.), R. C1001 (Trans.), *Climate Change 2014:*  
861 *Impacts, Adaptation, and Vulnerability. Part B: Regional Aspects. Contribution of Working*  
862 *Group II to the Fifth Assessment Report of the Intergovernmental Panel on Climate Change*  
863 (pp. 1655–1731). Cambridge, United Kingdom and New York, NY, USA: Cambridge  
864 University Press.
- 865 Hoegh-Guldberg, O., Jacob, D., Taylor, M., Guillén Bolaños, T., Bindi, M., Brown, S., ... Zhou,  
866 G. (2019). The human imperative of stabilizing global climate change at 1.5°C. *Science*,  
867 365(6459), eaaw6974. <https://doi.org/10.1126/science.aaw6974>
- 868 Hoogenboom, M. O., Connolly, S. R., & Anthony, K. R. N. (2008). Interactions between

869 morphological and physiological plasticity optimize energy acquisition in corals. *Ecology*,  
870 89(4), 1144–1154. <https://doi.org/10.1890/07-1272.1>

871 Hoogenboom, M., Rottier, C., Sikorski, S., & Ferrier-Pagès, C. (2015). Among-species variation  
872 in the energy budgets of reef-building corals: scaling from coral polyps to communities.  
873 *Journal of Experimental Biology*, 218(24), 3866–3877. <https://doi.org/10.1242/jeb.124396>

874 Houlbrèque, F., & Ferrier-Pagès, C. (2009). Heterotrophy in tropical scleractinian corals.  
875 *Biological Reviews*, 84(1), 1–17. <https://doi.org/10.1111/j.1469-185X.2008.00058.x>

876 Hughes, A., Grottoli, A., Pease, T., & Matsui, Y. (2010). Acquisition and assimilation of carbon  
877 in non-bleached and bleached corals. *Marine Ecology Progress Series*, 420, 91–101.  
878 <https://doi.org/10.3354/meps08866>

879 Hughes, T. P., Kerry, J. T., Álvarez-Noriega, M., Álvarez-Romero, J. G., Anderson, K. D.,  
880 Baird, A. H., ... Wilson, S. K. (2017). Global warming and recurrent mass bleaching of  
881 corals. *Nature*, 543(7645), 373–377. <https://doi.org/10.1038/nature21707>

882 Hughes, T. P., Kerry, J. T., Baird, A. H., Connolly, S. R., Chase, T. J., Dietzel, A., ... Woods, R.  
883 M. (2019, April 18). Global warming impairs stock–recruitment dynamics of corals. *Nature*.  
884 Nature Publishing Group. <https://doi.org/10.1038/s41586-019-1081-y>

885 Jackson, R. B., Le Quéré, C., Andrew, R. M., Canadell, J. G., Peters, G. P., Roy, J., & Wu, L.  
886 (2017). Warning signs for stabilizing global CO<sub>2</sub> emissions. *Environmental Research Letters*,  
887 12(11), 110202. <https://doi.org/10.1088/1748-9326/aa9662>

888 Jiang, L., Guo, Y.-J., Zhang, F., Zhang, Y.-Y., McCook, L. J., Yuan, X.-C., ... Huang, H.  
889 (2019). Diurnally fluctuating pCO<sub>2</sub> modifies the physiological responses of coral recruits  
890 under ocean acidification. *Frontiers in Physiology*, 9.  
891 <https://doi.org/10.3389/fphys.2018.01952>

892 Jones, A. M., & Berkelmans, R. (2011). Tradeoffs to thermal acclimation: energetics and  
893 reproduction of a reef coral with heat tolerant *Symbiodinium* Type-D. *Journal of Marine*  
894 *Biology*, 2011, 1–12. <https://doi.org/10.1155/2011/185890>

895 Kenkel, C. D., Meyer, E., & Matz, M. V. (2013). Gene expression under chronic heat stress in  
896 populations of the mustard hill coral (*Porites astreoides*) from different thermal

- 897 environments. *Molecular Ecology*, 22(16), 4322–4334. <https://doi.org/10.1111/mec.12390>
- 898 Kim, S. W., Sampayo, E. M., Sommer, B., Sims, C. A., Gómez-Cabrera, M. del C., Dalton, S. J.,  
899 ... Pandolfi, J. M. (2019). Refugia under threat: Mass bleaching of coral assemblages in  
900 high-latitude eastern Australia. *Global Change Biology*, 25(11), 3918–3931.  
901 <https://doi.org/10.1111/gcb.14772>
- 902 LaJeunesse, T., Bhagooli, R., Hidaka, M., deVantier, L., Done, T., Schmidt, G., ... Hoegh-  
903 Guldberg, O. (2004). Closely related *Symbiodinium* spp. differ in relative dominance in coral  
904 reef host communities across environmental, latitudinal and biogeographic gradients. *Marine*  
905 *Ecology Progress Series*, 284, 147–161. <https://doi.org/10.3354/meps284147>
- 906 Le Nohaïc, M., Ross, C. L., Cornwall, C. E., Comeau, S., Lowe, R., McCulloch, M. T., &  
907 Schoepf, V. (2017). Marine heatwave causes unprecedented regional mass bleaching of  
908 thermally resistant corals in northwestern Australia. *Scientific Reports*, 7(1), 14999.  
909 <https://doi.org/10.1038/s41598-017-14794-y>
- 910 Le Quéré, C., Andrew, R. M., Friedlingstein, P., Sitch, S., Hauck, J., Pongratz, J., ... Zheng, B.  
911 (2018). Global carbon budget 2018. *Earth System Science Data*, 10(4), 2141–2194.  
912 <https://doi.org/10.5194/essd-10-2141-2018>
- 913 Levas, S., Grottoli, A. G., Schoepf, V., Aschaffenburg, M., Baumann, J., Bauer, J. E., & Warner,  
914 M. E. (2016). Can heterotrophic uptake of dissolved organic carbon and zooplankton mitigate  
915 carbon budget deficits in annually bleached corals? *Coral Reefs*, 35(2), 495–506.  
916 <https://doi.org/10.1007/s00338-015-1390-z>
- 917 Levas, S. J., Grottoli, A. G., Hughes, A., Osburn, C. L., & Matsui, Y. (2013). Physiological and  
918 biogeochemical traits of bleaching and recovery in the mounding species of coral *Porites*  
919 *lobata*: Implications for resilience in mounding corals. *PLoS ONE*, 8(5).  
920 <https://doi.org/10.1371/journal.pone.0063267>
- 921 Lough, J. M., Anderson, K. D., & Hughes, T. P. (2018). Increasing thermal stress for tropical  
922 coral reefs: 1871–2017. *Scientific Reports*, 8(1), 6079. [https://doi.org/10.1038/s41598-018-](https://doi.org/10.1038/s41598-018-24530-9)  
923 [24530-9](https://doi.org/10.1038/s41598-018-24530-9)
- 924 Loya, Y., Sakai, K., Yamazato, K., Nakano, Y., Sambali, H., & van Woesik, R. (2001). Coral

- 925 bleaching: the winners and the losers. *Ecology Letters*, 4(2), 122–131.  
926 <https://doi.org/10.1046/j.1461-0248.2001.00203.x>
- 927 Manzello, D. P., Kleypas, J. A., Budd, D. A., Eakin, C. M., Glynn, P. W., & Langdon, C. (2008).  
928 Poorly cemented coral reefs of the eastern tropical Pacific: possible insights into reef  
929 development in a high-CO<sub>2</sub> world. *Proceedings of the National Academy of Sciences of the*  
930 *United States of America*, 105(30), 10450–5. <https://doi.org/10.1073/pnas.0712167105>
- 931 Manzello, D. P., Matz, M. V., Enochs, I. C., Valentino, L., Carlton, R. D., Kolodziej, G., ...  
932 Jankulak, M. (2018). Role of host genetics and heat tolerant algal symbionts in sustaining  
933 populations of the endangered coral *Orbicella faveolata* in the Florida Keys with ocean  
934 warming. *Global Change Biology*, 25(3), 1016–1031. <https://doi.org/10.1111/gcb.14545>
- 935 Marcelino, V. R., Morrow, K. M., van Oppen, M. J. H., Bourne, D. G., & Verbruggen, H.  
936 (2017). Diversity and stability of coral endolithic microbial communities at a naturally high  
937 pCO<sub>2</sub> reef. *Molecular Ecology*, 26(19), 5344–5357. <https://doi.org/10.1111/mec.14268>
- 938 Marshall, P. A. (2000). Skeletal damage in reef corals: relating resistance to colony morphology.  
939 *Marine Ecology Progress Series*, 200, 177–189. <https://doi.org/10.2307/24855870>
- 940 Marshall, P. A., & Baird, A. H. (2000). Bleaching of corals on the Great Barrier Reef:  
941 differential susceptibilities among taxa. *Coral Reefs*, 19(2), 155–163.  
942 <https://doi.org/10.1007/s003380000086>
- 943 Marubini, F., Ferrier-Pagès, C., Furla, P., & Allemand, D. (2008). Coral calcification responds to  
944 seawater acidification: a working hypothesis towards a physiological mechanism. *Coral*  
945 *Reefs*, 27(3), 491–499. <https://doi.org/10.1007/s00338-008-0375-6>
- 946 McCulloch, M., Falter, J., Trotter, J., & Montagna, P. (2012). Coral resilience to ocean  
947 acidification and global warming through pH up-regulation. *Nature Climate Change*, 2(8),  
948 623–627. <https://doi.org/10.1038/nclimate1473>
- 949 Meinshausen, M., Smith, S. J., Calvin, K., Daniel, J. S., Kainuma, M. L. T., Lamarque, J.-F., ...  
950 van Vuuren, D. P. P. (2011). The RCP greenhouse gas concentrations and their extensions  
951 from 1765 to 2300. *Climatic Change*, 109(1–2), 213–241. [https://doi.org/10.1007/s10584-](https://doi.org/10.1007/s10584-011-0156-z)  
952 [011-0156-z](https://doi.org/10.1007/s10584-011-0156-z)

- 953 Mellin, C., Matthews, S., Anthony, K. R. N., Brown, S. C., Caley, M. J., Johns, K. A., ...  
954 MacNeil, M. A. (2019). Spatial resilience of the Great Barrier Reef under cumulative  
955 disturbance impacts. *Global Change Biology*, 25(7), gcb.14625.  
956 <https://doi.org/10.1111/gcb.14625>
- 957 Mollica, N. R., Guo, W., Cohen, A. L., Huang, K. F., Foster, G. L., Donald, H. K., & Solow, A.  
958 R. (2018). Ocean acidification affects coral growth by reducing skeletal density. *Proceedings*  
959 *of the National Academy of Sciences of the United States of America*, 115(8), 1754–1759.  
960 <https://doi.org/10.1073/pnas.1712806115>
- 961 Muscatine, L., R. McCloskey, L., & E. Marian, R. (1981). Estimating the daily contribution of  
962 carbon from zooxanthellae to coral animal respiration. *Limnology and Oceanography*, 26(4),  
963 601–611. <https://doi.org/10.4319/lo.1981.26.4.0601>
- 964 National Oceanic and Atmospheric Administration Coral Reef Watch. 5-km pixel satellite data.  
965 Available at: <https://coralreefwatch.noaa.gov/satellite/index.php>
- 966 Palardy, J. E., Rodrigues, L. J., & Grottoli, A. G. (2008). The importance of zooplankton to the  
967 daily metabolic carbon requirements of healthy and bleached corals at two depths. *Journal of*  
968 *Experimental Marine Biology and Ecology*, 367(2), 180–188.  
969 <https://doi.org/10.1016/j.jembe.2008.09.015>
- 970 Palardy, J., Grottoli, A., & Matthews, K. (2005). Effects of upwelling, depth, morphology and  
971 polyp size on feeding in three species of Panamanian corals. *Marine Ecology Progress Series*,  
972 300, 79–89. <https://doi.org/10.3354/meps300079>
- 973 Pandolfi, J. M., Connolly, S. R., Marshall, D. J., & Cohen, A. L. (2011). Projecting coral reef  
974 futures under global warming and ocean acidification. *Science*, 333(6041), 418–422.  
975 <https://doi.org/10.1126/science.1204794>
- 976 Perry, C. T., Steneck, R. S., Murphy, G. N., Kench, P. S., Edinger, E. N., Smithers, S. G., &  
977 Mumby, P. J. (2015). Regional-scale dominance of non-framework building corals on  
978 Caribbean reefs affects carbonate production and future reef growth. *Global Change Biology*,  
979 21(3), 1153–1164. <https://doi.org/10.1111/gcb.12792>
- 980 Peters, G. P., Le Quéré, C., Andrew, R. M., Canadell, J. G., Friedlingstein, P., Ilyina, T., ...

- 981 Tans, P. (2017). Towards real-time verification of CO<sub>2</sub> emissions. *Nature Climate Change*,  
982 7(12), 848–850. <https://doi.org/10.1038/s41558-017-0013-9>
- 983 Reyes-Nivia, C., Diaz-Pulido, G., Kline, D., Guldberg, O.-H., & Dove, S. (2013). Ocean  
984 acidification and warming scenarios increase microbioerosion of coral skeletons. *Global*  
985 *Change Biology*, 19(6), 1919–1929. <https://doi.org/10.1111/gcb.12158>
- 986 Reynaud, S., Leclercq, N., Romaine-Lioud, S., Ferrier-Pages, C., Jaubert, J., & Gattuso, J.-P.  
987 (2003). Interacting effects of CO<sub>2</sub> partial pressure and temperature on photosynthesis and  
988 calcification in a scleractinian coral. *Global Change Biology*, 9(11), 1660–1668.  
989 <https://doi.org/10.1046/j.1365-2486.2003.00678.x>
- 990 Riegl, B., Johnston, M., Purkis, S., Howells, E., Burt, J., Steiner, S. C. C., ... Bauman, A. (2018).  
991 Population collapse dynamics in *Acropora downingi*, an Arabian/Persian Gulf ecosystem-  
992 engineering coral, linked to rising temperature. *Global Change Biology*, 24(6), 2447–2462.  
993 <https://doi.org/10.1111/gcb.14114>
- 994 Rivest, E. B., Comeau, S., & Cornwall, C. E. (2017, December 1). The role of natural variability  
995 in shaping the response of coral reef organisms to climate change. *Current Climate Change*  
996 *Reports*. Springer. <https://doi.org/10.1007/s40641-017-0082-x>
- 997 Rodolfo-Metalpa, R., Hoogenboom, M. O., Rottier, C., Ramos-Esplá, A., Baker, A. C., Fine, M.,  
998 & Ferrier-Pagès, C. (2014). Thermally tolerant corals have limited capacity to acclimatize to  
999 future warming. *Global Change Biology*, 20(10), 3036–3049.  
1000 <https://doi.org/10.1111/gcb.12571>
- 1001 Rodrigues, L. J., & Grottoli, A. G. (2007). Energy reserves and metabolism as indicators of coral  
1002 recovery from bleaching. *Limnology and Oceanography*, 52(5), 1874–1882.  
1003 <https://doi.org/10.4319/lo.2007.52.5.1874>
- 1004 Safaie, A., Silbiger, N. J., McClanahan, T. R., Pawlak, G., Barshis, D. J., Hench, J. L., ... Davis,  
1005 K. A. (2018). High frequency temperature variability reduces the risk of coral bleaching.  
1006 *Nature Communications*, 9(1), 1671. <https://doi.org/10.1038/s41467-018-04074-2>
- 1007 Sampayo, E. M., Ridgway, T., Bongaerts, P., & Hoegh-Guldberg, O. (2008). Bleaching  
1008 susceptibility and mortality of corals are determined by fine-scale differences in symbiont

- 1009 type. *Proceedings of the National Academy of Sciences of the United States of America*,  
1010 105(30), 10444–10449. <https://doi.org/10.1073/pnas.0708049105>
- 1011 Schoepf, V., Carrion, S. A., Pfeifer, S. M., Naugle, M., Dugal, L., Bruyn, J., & McCulloch, M. T.  
1012 (2019). Stress-resistant corals may not acclimatize to ocean warming but maintain heat  
1013 tolerance under cooler temperatures. *Nature Communications*, 10(1), 4031.  
1014 <https://doi.org/10.1038/s41467-019-12065-0>
- 1015 Schoepf, V., Grottoli, A. G., Levas, S. J., Aschaffenburg, M. D., Baumann, J. H., Matsui, Y., &  
1016 Warner, M. E. (2015). Annual coral bleaching and the long-term recovery capacity of coral.  
1017 *Proceedings of the Royal Society B: Biological Sciences*, 282(1819).  
1018 <https://doi.org/10.1098/rspb.2015.1887>
- 1019 Schoepf, V., Grottoli, A. G., Warner, M. E., Cai, W.-J., Melman, T. F., Hoadley, K. D., ...  
1020 Baumann, J. H. (2013). Coral energy reserves and calcification in a high-CO<sub>2</sub> world at two  
1021 temperatures. *PLoS ONE*, 8(10), e75049. <https://doi.org/10.1371/journal.pone.0075049>
- 1022 Schoepf, V., Levas, S. J., Rodrigues, L. J., McBride, M. O., Aschaffenburg, M. D., Matsui, Y.,  
1023 ... Grottoli, A. G. (2014). Kinetic and metabolic isotope effects in coral skeletal carbon  
1024 isotopes: A re-evaluation using experimental coral bleaching as a case study. *Geochimica et*  
1025 *Cosmochimica Acta*, 146, 164–178. <https://doi.org/10.1016/j.gca.2014.09.033>
- 1026 Shashar, N., Banaszak, A., Lesser, M., & Amrami, D. (1997). Coral endolithic algae: life in a  
1027 protected environment. *Pacific Science*, 51(2), 167–173. Retrieved from  
1028 <http://scholarspace.manoa.hawaii.edu/bitstream/10125/3107/1/v51n2-167-173.pdf>
- 1029 Shaw, E. C., McNeil, B. I., Tilbrook, B., Matear, R., & Bates, M. L. (2013). Anthropogenic  
1030 changes to seawater buffer capacity combined with natural reef metabolism induce extreme  
1031 future coral reef CO<sub>2</sub> conditions. *Global Change Biology*, 19(5), 1632–1641.  
1032 <https://doi.org/10.1111/gcb.12154>
- 1033 Siebeck, U. E., Marshall, N. J., Klüter, A., & Hoegh-Guldberg, O. (2006). Monitoring coral  
1034 bleaching using a colour reference card. *Coral Reefs*, 25(3), 453–460.  
1035 <https://doi.org/10.1007/s00338-006-0123-8>
- 1036 Spencer Davies, P. (1989). Short-term growth measurements of corals using an accurate buoyant



- 1037 weighing technique. *Marine Biology*, 101(3), 389–395. <https://doi.org/10.1007/BF00428135>
- 1038 Sully, S., Burkepile, D. E., Donovan, M. K., Hodgson, G., & van Woesik, R. (2019). A global  
1039 analysis of coral bleaching over the past two decades. *Nature Communications*, 10(1), 1264.  
1040 <https://doi.org/10.1038/s41467-019-09238-2>
- 1041 Tambutté, E., Venn, A. A., Holcomb, M., Segonds, N., Techer, N., Zoccola, D., ... Tambutté, S.  
1042 (2015). Morphological plasticity of the coral skeleton under CO<sub>2</sub>-driven seawater  
1043 acidification. *Nature Communications*, 6, 7368. <https://doi.org/10.1038/ncomms8368>
- 1044 Tolosa, I., Treignier, C., Grover, R., & Ferrier-Pagès, C. (2011). Impact of feeding and short-  
1045 term temperature stress on the content and isotopic signature of fatty acids, sterols, and  
1046 alcohols in the scleractinian coral *Turbinaria reniformis*. *Coral Reefs*, 30(3), 763–774.  
1047 <https://doi.org/10.1007/s00338-011-0753-3>
- 1048 Tremblay, P., Ferrier-Pagès, C., Maguer, J. F., Rottier, C., Legendre, L., & Grover, R. (2012).  
1049 Controlling effects of irradiance and heterotrophy on carbon translocation in the temperate  
1050 coral *Cladocora caespitosa*. *PLoS ONE*, 7(9), e44672.  
1051 <https://doi.org/10.1371/journal.pone.0044672>
- 1052 Tremblay, P., Gori, A., Maguer, J. F., Hoogenboom, M., & Ferrier-Pagès, C. (2016).  
1053 Heterotrophy promotes the re-establishment of photosynthate translocation in a symbiotic  
1054 coral after heat stress. *Scientific Reports*, 6, 38112. <https://doi.org/10.1038/srep38112>
- 1055 Underwood, A. (1997). *Experiments in ecology: their logical design and interpretation using*  
1056 *analysis of variance*. Cambridge University Press.  
1057 <https://doi.org/10.1017/S0025315400072064>
- 1058 van Hooijdonk, R., Maynard, J., Tamelander, J., Gove, J., Ahmadi, G., Raymundo, L., ...  
1059 Planes, S. (2016). Local-scale projections of coral reef futures and implications of the Paris  
1060 Agreement. *Scientific Reports*, 6(1), 39666. <https://doi.org/10.1038/srep39666>
- 1061 van Vuuren, D. P., Edmonds, J., Kainuma, M., Riahi, K., Thomson, A., Hibbard, K., ... Rose, S.  
1062 K. (2011). The representative concentration pathways: an overview. *Climatic Change*, 109(1–  
1063 2), 5–31. <https://doi.org/10.1007/s10584-011-0148-z>
- 1064 van Woesik, R., Golbuu, Y., & Roff, G. (2015). Keep up or drown: Adjustment of western

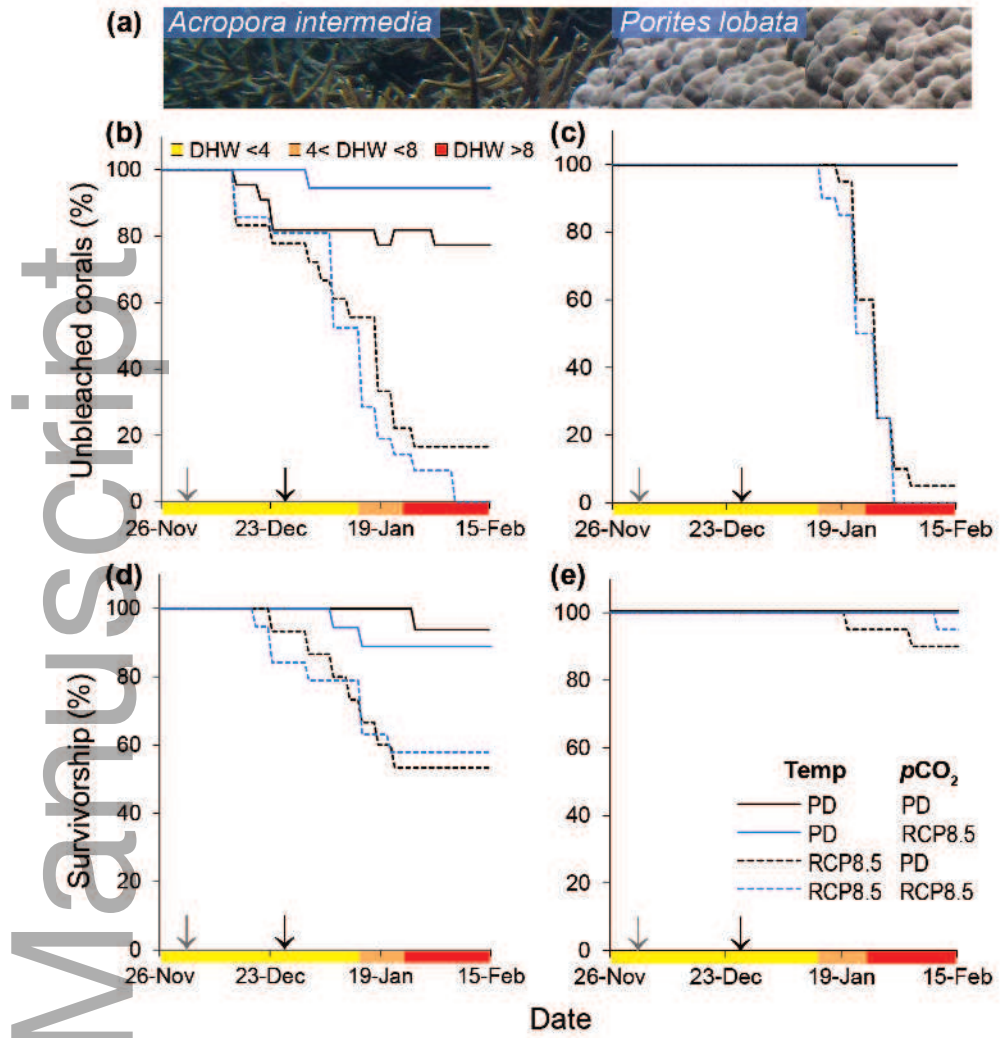
- 1065 Pacific coral reefs to sea-level rise in the 21st century. *Royal Society Open Science*, 2(7).  
1066 <https://doi.org/10.1098/rsos.150181>
- 1067 Veal, C. J., Carmi, M., Fine, M., & Hoegh-Guldberg, O. (2010). Increasing the accuracy of  
1068 surface area estimation using single wax dipping of coral fragments. *Coral Reefs*, 29(4), 893–  
1069 897. <https://doi.org/10.1007/s00338-010-0647-9>
- 1070 Venn, A. A., Tambutté, E., Holcomb, M., Laurent, J., Allemand, D., & Tambutté, S. (2013).  
1071 Impact of seawater acidification on pH at the tissue-skeleton interface and calcification in reef  
1072 corals. *Proceedings of the National Academy of Sciences of the United States of America*,  
1073 110(5), 1634–1639. <https://doi.org/10.1073/pnas.1216153110>
- 1074 Wahl, M., Saderne, V., & Sawall, Y. (2016). How good are we at assessing the impact of ocean  
1075 acidification in coastal systems? Limitations, omissions and strengths of commonly used  
1076 experimental approaches with special emphasis on the neglected role of fluctuations. *Marine  
1077 and Freshwater Research*, 67(1), 25. <https://doi.org/10.1071/MF14154>
- 1078 Wall, C. B., Mason, R. A. B., Ellis, W. R., Cunning, R., & Gates, R. D. (2017). Elevated  $p\text{CO}_2$   
1079 affects tissue biomass composition, but not calcification, in a reef coral under two light  
1080 regimes. *Royal Society Open Science*, 4(11), 170683. <https://doi.org/10.1098/rsos.170683>
- 1081 Wall, M., Fietzke, J., Schmidt, G. M., Fink, A., Hofmann, L. C., de Beer, D., & Fabricius, K. E.  
1082 (2016). Internal pH regulation facilitates in situ long-term acclimation of massive corals to  
1083 end-of-century carbon dioxide conditions. *Scientific Reports*, 6(1), 30688.  
1084 <https://doi.org/10.1038/srep30688>
- 1085 Whitaker, J. R., & Granum, P. E. (1980). An absolute method for protein determination based on  
1086 difference in absorbance at 235 and 280 nm. *Analytical Biochemistry*, 109(1), 156–159.  
1087 [https://doi.org/10.1016/0003-2697\(80\)90024-X](https://doi.org/10.1016/0003-2697(80)90024-X)
- 1088 Wolff, N. H., Mumby, P. J., Devlin, M., & Anthony, K. R. N. (2018). Vulnerability of the Great  
1089 Barrier Reef to climate change and local pressures. *Global Change Biology*, 24(5), 1978–  
1090 1991. <https://doi.org/10.1111/gcb.14043>
- 1091 Wright, R. M., Mera, H., Kenkel, C. D., Nayfa, M., Bay, L. K., & Matz, M. V. (2019). Positive  
1092 genetic associations among fitness traits support evolvability of a reef-building coral under

1093 multiple stressors. *Global Change Biology*, 25(10), 3294–3304.  
1094 <https://doi.org/10.1111/gcb.14764>

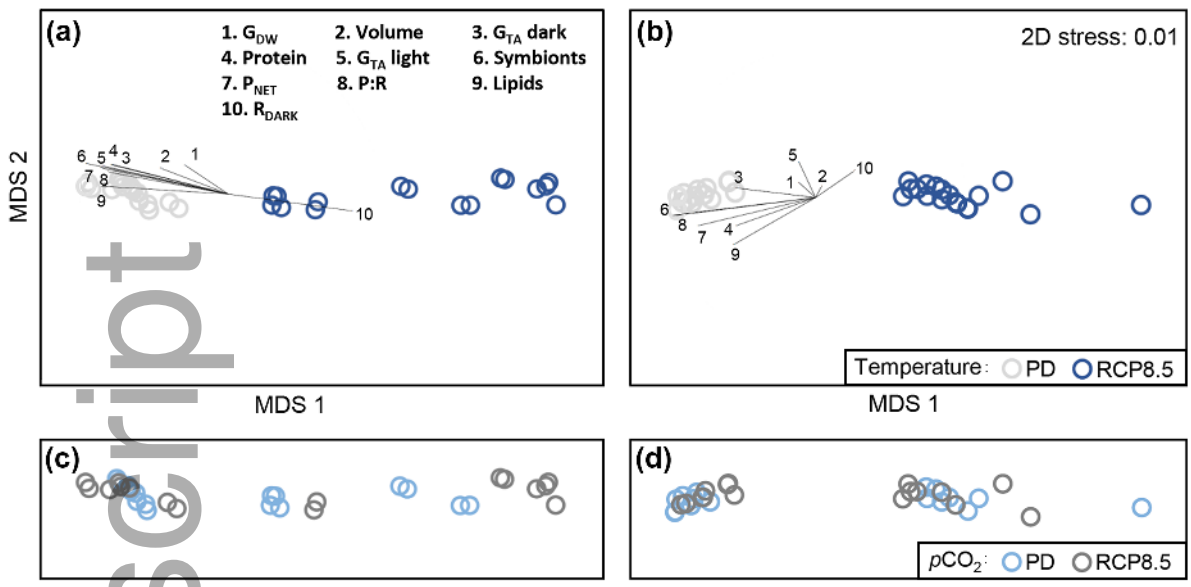
1095 Ziegler, M., Grupstra, C. G. B., Barreto, M. M., Eaton, M., BaOmar, J., Zubier, K., ... Voolstra,  
1096 C. R. (2019). Coral bacterial community structure responds to environmental change in a  
1097 host-specific manner. *Nature Communications*, 10(1). [https://doi.org/10.1038/s41467-019-](https://doi.org/10.1038/s41467-019-10969-5)  
1098 10969-5

1099 Ziegler, M., Seneca, F. O., Yum, L. K., Palumbi, S. R., & Voolstra, C. R. (2017). Bacterial  
1100 community dynamics are linked to patterns of coral heat tolerance. *Nature Communications*,  
1101 8. <https://doi.org/10.1038/ncomms14213>

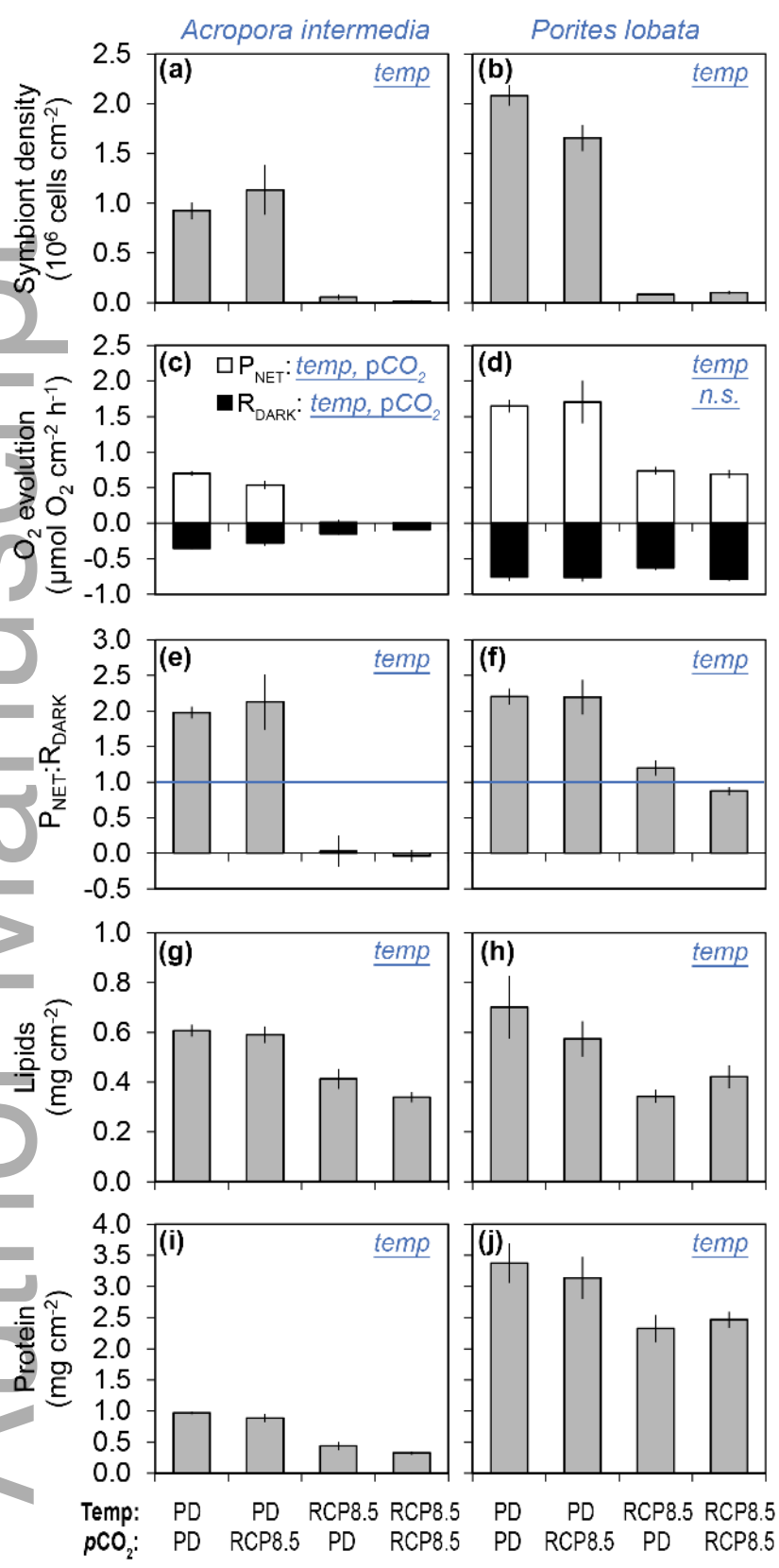
Author Manuscript



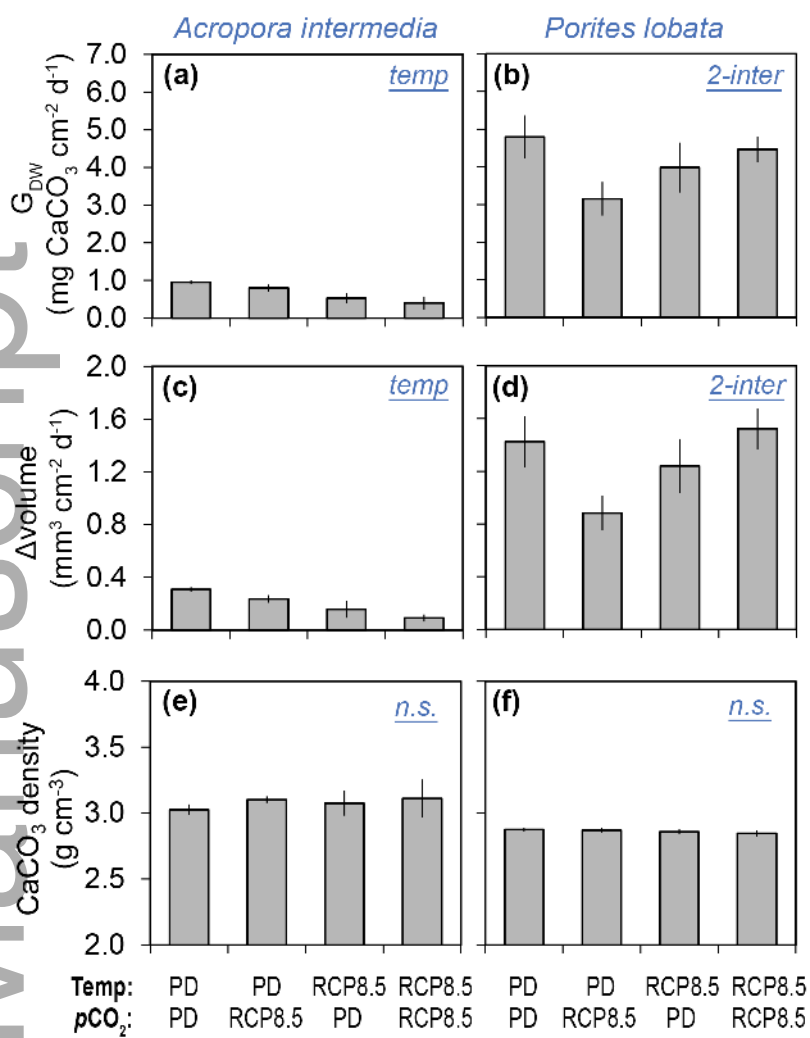
gcb\_14998\_f1.tif



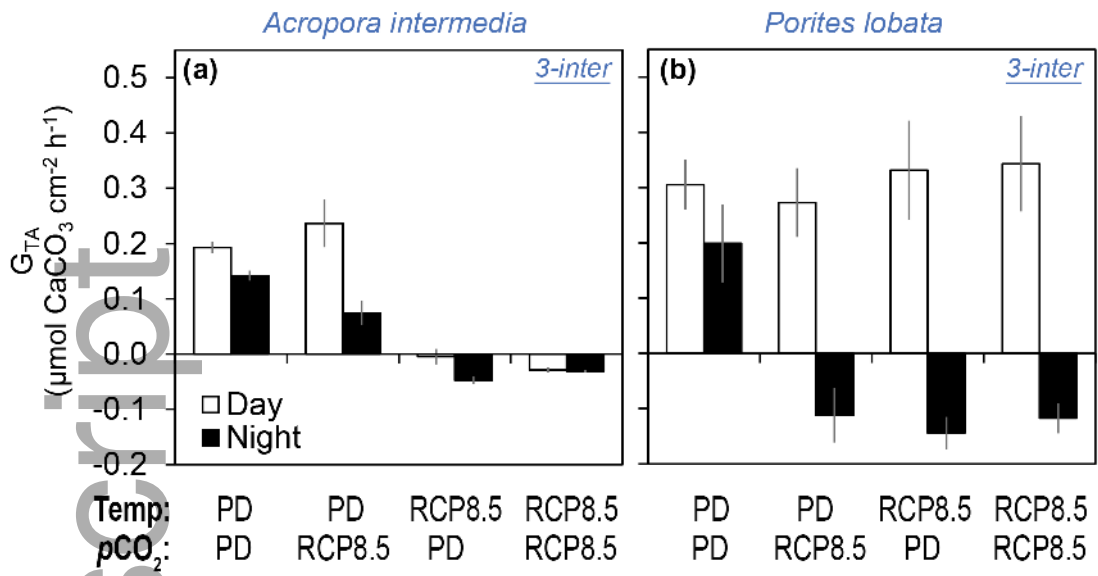
gcb\_14998\_f2.tif



gcb\_14998\_f3.tif



gcb\_14998\_f4.tif



gcb\_14998\_f5.tif